2-5-2018

Reaction Chemistry of Silver(I) Trifluoromethanesulfonate Complexes of Nitrogen-Confused *C*-Scorpionates

James R. Gardinier
Marquette University, james.gardinier@marquette.edu

Kristin J. Meise
Marquette University

Fathiya Jahan
Marquette University

Sergey V. Lindeman
Marquette University, sergey.lindeman@marquette.edu

Accepted version. *Inorganic Chemistry,* Vol. 57, No. 3 (February 5, 2018): DOI.

Inorganic Chemistry, Vol. 57, No. 3 (2018): 1572-1589. DOI.

Tapping Environmental History to Recreate America's Colonial Hydrology

James R. Gardinier
Department of Chemistry, Marquette University, Milwaukee, WI
Kristin J. Meise
Department of Chemistry, Marquette University, Milwaukee, WI
Fathiya Jahan
Department of Chemistry, Marquette University, Milwaukee, WI
Sergey V. Lindeman
Department of Chemistry, Marquette University, Milwaukee, WI

Abstract

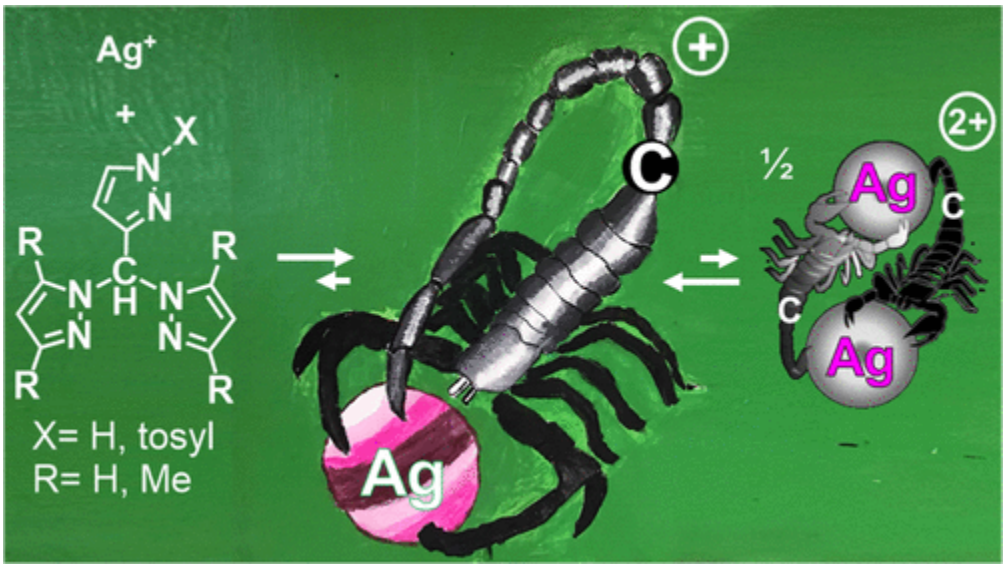

Two new *C*-scorpionate ligands with a bis(3,5-dimethylpyrazol-1-yl)methyl group bound to the 3 position of either an *N*-tosyl (^{Ts}L*) or an N–H pyrazole (^{H}L*) ring have been prepared. The silver(I) complexes of these new ligands and the two previously reported analogous ligands with unsubstituted bis(pyrazol-1-yl)methyl groups (^{Ts}L and ^{H}L) in both 1:1 and 2:1 ligand/metal ratios were investigated to explore the effects of ligand sterics on their physical and chemical properties. The structurally characterized derivatives of the type [Ag(L)$_2$](OTf) are four-coordinate, where the confused pyrazolyl is not bound to the metal. On the other hand, three 1:1 complexes [Ag(L)](OTf) had all pyrazolyls bound, while the μ–κ^1,κ^1-^{Ts}L derivative had an unbound confused pyrazolyl. The molecularity of the latter four ranged from polymeric to dimeric to monomeric in the solid with increasing steric bulk of the ligand. The utility of these complexes in stoichiometric ligand-transfer reactions and in styrene aziridination was demonstrated. Thus, tricarbonylmanganese(I) complexes were prepared as kinetically inert models for comparative solution diffusion NMR studies. Also, [Fe(^{H}L)$_2$](OTf)$_2$ was prepared for similar reasons and to compare the effects of anion on spin-crossover properties.

Introduction

Scorpionate ligands, which originally referred to Trofimenko's tris(pyrazolyl)borates, Tp^x,[(1)] are ubiquitous in modern coordination chemistry. The "scorpionate" moniker is also used to classify other facial trichelating ligands[(1b)] such as Reglinski's tris(thioimidazolyl)borate, Tm^R (aka "soft" scorpionates),[(2)] and *C*-scorpionate counterparts such as tris(pyrazolyl)methane, Tpm^x,[(3)] and tris(pyrazolyl)methanesulfonate, Tpms.[(4)] The chemistry of silver(I) scorpionates has seen tremendous growth in the last 15 years, ever since the subject was first reviewed.[(5, 6)] At the time of the 2004 review, the chemistry of these derivatives was still in its infancy because first-generation scorpionates with B–H bonds had a proclivity for reducing silver(I) to the metal. It was learned in the late 1990s that silver reduction could be slowed by increasing the steric bulk on the pyrazolyls, by removing B–H bonds, and/or by introducing electron-withdrawing groups on the pyrazolyl rings.[(6)] Intensified interest in silver(I) scorpionates began with early reports from the Dias group that showed that the fluorinated scorpionate complex, AgTp$^{(CF_3)_2}$, was a competent catalyst for carbene insertion into C–halogen bonds,[(7)] aromatic

C═C bonds (Büchner reaction),[8] and aliphatic C–H bonds.[9] Further inciting interest were reports from the Pérez group that showed that $AgTp^x$ complexes catalyzed a variety of transformations[6] such as carbene insertion into alkane C–H bonds,[10] Si–H bonds,[11] and C–X (X = Cl, Br) bonds[12] or were used for the cross-coupling of diazo compounds.[13] Moreover, diverse $AgTp^x$-catalyzed nitrene-transfer reactions have been discovered such as aziridination of alkenes[14] and dienes,[15] amination of alkanes,[16] and unexpected N–N bond formations.[17] More recently, other silver scorpionates, such as Huang's $Ag(PPh_3)(^{Ph}Tm)$[18] and Perez's $Ag[PhB(CH_2PPh_2)_3](PPh_3)$,[19] were also found to catalyze the aziridination of styrene, albeit in much lower yields than the analogous copper complexes.

In contrast to the $AgTp^x$ and other anionic *B*-scorpionates, the reaction and catalytic chemistry of AgTpms[20] or $[Ag_n(Tpm^x)_m]^+$ [21, 22] remains largely unreported. The chemistry of $[Ag_n(Tpm^x)_m]^+$ compounds lagged behind the Tp^x derivatives in part because of difficulties in the original ligand synthesis,[23] which were only resolved in 1984 by Elguero and co-workers.[24] Large-scale syntheses and subsequent functionalization chemistry of tris(pyrazolyl)methanes were then introduced in 2000.[25] These breakthroughs opened the door for countless new variations including Tpms.[4] Given the remarkable achievements reported by various groups in the use of silver complexes of charge-neutral nitrogen donors to effect both aziridination and amination reactions,[24-29] similar chemistry might be expected for tris(pyrazolyl)methanes but, surprisingly, has not yet been reported for this metal.[30]

Our group has recently introduced a new class of tris(pyrazolyl)methanes, the nitrogen-confused *C*-scorpionates,[31] where one of the three pyrazolyl rings is bound to the central methine carbon atom via a pyrazolyl ring carbon atom rather than the more usual nitrogen atom (Figure 1). With this mode of linkage, easy access to variable steric and electronic properties of the ligands can be gained by any variety of simple nitrogen protection and deprotection reactions. Importantly, by a suitable choice of the confused pyrazolyl's X group, it should be possible to promote favorable supramolecular interactions in the second coordination sphere of a complex to either guide crystallization or facilitate reactions. In this contribution, the preparation of new nitrogen-confused *C*-scorpionate ligands with two "normal" pz* groups (=3,5-dimethylpyrazol-1yl) and a "confused" pyrazolyl with either N–H, $^{H}L^*$, or *N*-Tosyl (Tosyl = *p*-toluenesulfonyl), $^{Ts}L^*$, bound to a central methine carbon atom is described. These bulky ligands complement those previously described, ^{H}L and ^{Ts}L, which had less bulky, unsubstituted, "normal" pyrazol-1-yls. For these four related nitrogen-confused scorpionate ligands, the 2:1 and 1:1 ligand/silver complexes are prepared and characterized both structurally and spectroscopically. The complexes' stoichiometric reactivity and catalytic activity for aziridination of styrene are also reported.

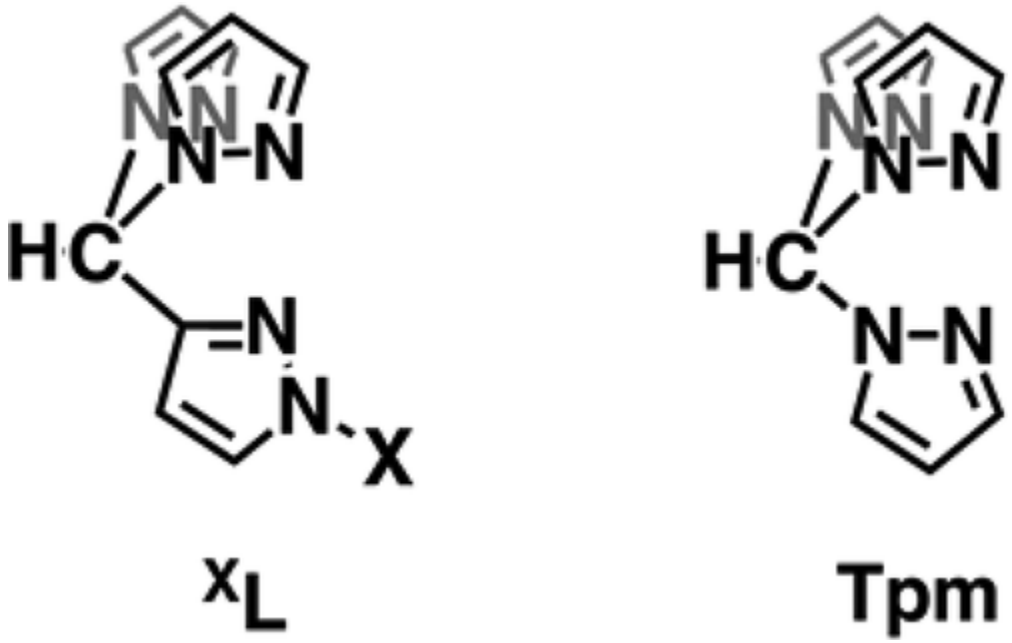

Figure 1. Depiction of “nitrogen-confused” *C*-scorpionates [left; X = H, Bz = $CH_2C_6H_5$, Ts = SO_2(*p*-tolyl)] versus the “normal” *C*-scorpionate, tris(pyrazolyl)methane, Tpm (right).

Experimental Section

General Considerations

The compounds (*p*-$CH_3C_6H_4SO_2$═Ts)pzC(O)H, ^{Ts}pzCHpz$_2$ (^{Ts}L), and ^{H}pzCHpz$_2$ (^{H}L) were prepared as described previously.[(31)] The compound O═C(pz*)$_2$ was prepared by the literature method.[(32)] Anhydrous $CoCl_2$, AgOTf (OTf = trifluoromethanesulfonate), $Mn(CO)_5Br$, Fe, $Fe(OTf)_2$, $FeCl_2$, $PhI(OAc)_2$, H_2NTs, and styrene were purchased from commercial sources and used as received. Anhydrous $Fe(OTf)_2$, $CoCl_2$, and AgOTf were stored under argon in a drybox. Commercial solvents were dried by conventional means and distilled under a nitrogen atmosphere prior to use. The silver(I), manganese(I), and iron(II) complexes were prepared under argon using Schlenk-line techniques, however, after isolation, were stored and manipulated under normal laboratory atmospheric conditions, unless otherwise specified (see the Nitrene-Transfer Catalysis section).

Instrumentation

Midwest MicroLab, LLC (Indianapolis, IN), performed all elemental analyses. Melting point determinations were made on samples contained in glass capillaries using an Electrothermal 9100 apparatus and are uncorrected. IR spectra were recorded for samples as KBr pellets or as either solutions or Nujol mulls between KBr plates in the 4000–500 cm^{-1} region on a Nicolet Magna-IR 560 spectrometer or on solid samples using a Thermo Scientific Nicolet iS5 IR spectrometer equipped with an iD3 attenuated-total-reflection (ATR) accessory. ^{1}H, ^{13}C, and ^{19}F NMR spectra were recorded on a Varian 400 MHz spectrometer. Chemical shifts were referenced to solvent resonances at δ_H 7.26 and δ_C 77.23 for $CDCl_3$ or δ_H 1.94 and δ_C 118.26 for CD_3CN. Details regarding the diffusion-oriented NMR experiments are found in the Supporting Information. Abbreviations for NMR and UV–vis: br (broad), sh (shoulder), m

(multiplet), ps (pseudo-), s (singlet), d (doublet), t (triplet), q (quartet), p (pentet), sept (septet). The solution magnetic moment was measured by Evan's method.[33] Magnetic susceptibility data were collected on a Quantum Design MPMS3 SQUID magnetometer. Raw moment data were corrected for the sample shape and radial offset corrections using the MPMS 3 Sample Geometry Simulator.[34] Diamagnetic corrections of -218×10^{-6} emu/mol for **9**, calculated from tabulated Pascal's constants,[35] were applied to the measured susceptibility data, as appropriate. Electronic absorption (UV–vis/near-IR) measurements were made on a Cary 5000 instrument. Powder X-ray diffraction patterns were collected with a Rigaku MiniFlex II instrument using Cu Kα (1.54178 Å) radiation. Positive-mode electrospray ionization mass spectrometry [ESI(+) MS] measurements were obtained on a Micromass Q-TOF spectrometer where formic acid (ca. 0.1% v/v) was added to the mobile phase (CH_3CN).

Ligands

TspzCHpz*2 (TsL*)

A mixture of 2.132 g (8.511 mmol) of ^{Ts}pzC(O)H, 2.092 g (9.585 mmol) of O═C(pz*)$_2$, and 0.055 g (0.43 mmol) of $CoCl_2$ in 50 mL of toluene was heated at reflux for 16 h. The resulting blue mixture was cooled to room temperature, and the solvent was removed by vacuum distillation. The residue was partitioned between 100 mL of water (H_2O) and 100 mL of ethyl acetate (EtOAc). The layers were separated, and the aqueous layer was extracted with two 50 mL portions of CH_2Cl_2. The organic fractions were combined, dried over $MgSO_4$, and filtered. Solvents were removed by vacuum distillation to leave 3.29 g (91%) of ^{Ts}L* as a pale-yellow solid. Recrystallization by cooling a boiling supersaturated solution in methanol (MeOH) to room temperature gave crystalline ivory-tinted blocks (ca. 25 mg/mL) after filtration and drying under vacuum. Mp: 181–182 °C. IR (CH_2Cl_2, KBr): ν_{CH} 3141, 2971, 2856. IR (ATR, cm^{-1}): ν_{CH} 3195, 3163, 3146, 3051, 2973, 2923, ν_{SO} 1374 (asym), 1179 (sym). ^{1}H NMR (CD_3CN): δ_H 8.19 (d, J = 2.8 Hz, 1 H, H_{5cpz}), 7.81 (d, J = 8.4 Hz, 2 H, Ts), 7.48 (s, 1 H, $H_{methine}$), 7.41 (d, J = 8.4 Hz, 2 H, Ts), 6.35 (d, J = 2.8 Hz, 1 H, H_{4cpz}), 5.83 (s, 2 H, H_{4pz*}), 2.42 (s, 3 H, TsCH_3), 2.07 (s, 6 H, pz*CH_3), 2.05 (s, 6 H, pz*CH_3). ^{13}C NMR (CD_3CN): δ_C 155.42, 149.14, 147.85, 141.71, 134.64, 133.72, 131.23, 128.84, 110.98 (C_{4cpz}), 107.56 (C_{4pz*}), 69.44 ($C_{methine}$), 21.71 (TsMe), 13.61 (pz*Me), 11.44 (pz*Me).

HpzCHpz*2 (HL*)

A solution of 15.0 mL of 5.00 M NaOH(aq) (75.0 mmol), 3.29 g (7.75 mmol) of ^{Ts}L*, and 20 mL of tetrahydrofuran (THF) was heated at reflux for 1.25 h. The solution was allowed to cool to room temperature and then extracted with two 50 mL portions of EtOAc. The organic fractions were dried over $MgSO_4$ and filtered. The organic solvent was removed by vacuum distillation, and the residue was triturated with diethyl ether (Et_2O) to leave 1.61 g (77%) of ^{H}L* as a colorless solid. Mp: 146–147 °C. IR (CH_2Cl_2, KBr): ν_{NH} 3450, ν_{CH} 3054 2986, 2857. IR (ATR, cm^{-1}): ν_{CH} 3141, 3051, 2971, 2956, 2914. ^{1}H NMR (CD_3CN): δ_H 11.25 (br s, 1 H, N–H), 7.56 (d, J = 2.3 Hz, 1 H, H_{5cpz}), 7.55 (s, 1 H, $H_{methine}$), 6.15 (d, J = 2.3 Hz, 1 H, H_{4cpz}), 5.86 (s, 2 H, H_{4pz*}), 2.21 (s, 6 H, pz*CH_3), 2.07 (s, 6 H, pz*CH_3). ^{13}C NMR ($CDCl_3$): δ_C 148.95, 141.59, 107.19 (C_{4pz*}), 106.11 (C_{4cpz}), 69.20 ($C_{methine}$), 13.65 (pz*Me), 11.52 (pz*Me); two resonances presumably for quartenary pyrazolyl carbon atoms are not observed.

Silver Complexes

General Procedure

A solution of a given ligand (ca. 0.5–2.0 mmol) in 10 mL of THF was added to a solution of AgOTf (1 or 0.5 equiv) in 10 mL of THF by cannula transfer. The flask originally containing the ligand was washed twice with 2 mL of THF, and the washings were transferred to the reaction medium to ensure quantitative transfer of the reagent. After the mixture had been stirred overnight for 14 h, the colorless precipitate was collected after cannula filtration, washing the solid with two 2 mL portions of Et_2O and drying under vacuum for 30 min. The quantities of the reagents used and of the products obtained and characterization data for each of the eight new compounds are given below. An alternative workup in the case where no precipitate was observed (complex **4b**) is also described.

[Ag(^{Ts}L*)](OTf) (**1a**)

A mixture of 0.306 g (0.721 mmol) of ^{Ts}L* and 0.185 g (0.720 mmol) of AgOTf gave 0.333 g (68%) of **1a** as a colorless solid after drying under vacuum at 100 °C for 4 h. Mp: 183–185 °C (dec). Anal. Calcd (found) for $C_{22}H_{24}N_6AgF_3O_5S_2$: C, 38.78 (39.05); H, 3.55 (3.73); N, 12.33 (12.15). IR (ATR, cm^{-1}): tosyl, 1393 (ν_{as}, SO_2), 911 ($\nu_{S–N}$); triflate (s to vs), 1260 (ν_{as}, SO_3), 1223 (ν_s, CF_3), 1162 (ν_{as}, CF_3), 1029 (ν_s, SO_3), 638 (δ_s, SO_3). ^{1}H NMR (CD_3CN): δ_H 8.20 (d, *J* = 2.8 Hz, 1 H, H_{5cpz}), 7.78 (d, *J* = 8.5 Hz, 2 H, Ts), 7.46 (s, 1 H, $H_{methine}$), 7.41 (d, *J* = 8.5 Hz, 2 H, Ts), 6.11 (d, *J* = 2.8 Hz, 1 H, H_{4cpz}), 6.04 (s, 2 H, H_{4pz*}), 2.42 (s, 3 H, $TsCH_3$), 2.41 (s, 6 H, pz*CH_3), 1.94 (s, 6 H, pz*CH_3). ^{13}C NMR (CD_3CN): δ_C 154.56, 151.93, 147.93, 143.85, 134.55, 134.10, 131.27, 128.87, 110.48 (C_{4cpz}), 107.32 (C_{4pz*}), 65.11 ($C_{methine}$), 21.75 (TsMe), 14.06 (pz*Me), 11.36 (pz*Me). ^{19}F NMR (CD_3CN): δ_F −79.32 (s). ESI(+) MS (relative intensity) assignment: *m*/*z* 957 (73) [Ag(^{Ts}L*)$_2$]$^+$, 531 (36) [Ag(^{Ts}L*)]$^+$, 447 (7) [Na(**^{Ts}L***)]$^+$, 425 (5) [H(^{Ts}L*)]$^+$, 329 (100) [^{Ts}L* – Hpz*]$^+$. A sample that was dried under vacuum for 30 min without heating analyzed as **3b**·THF. Anal. Calcd (found) for $C_{26}H_{32}N_6AgF_3O_4S$: C, 41.49 (41.39); H, 4.28 (4.19); N, 11.15 (11.23). X-ray-quality single crystals of mostly **1a** and some larger plates of **1b**·MeOH were grown by vapor diffusion of Et_2O into a MeOH solution (1.3 mL, 0.005 M).

[Ag(^{Ts}L*)$_2$](OTf) (**1b**)

A mixture of 0.250 g (0.589 mmol) of **^{Ts}L*** and 0.0757 g (0.295 mmol) of Ag(OTf) gave 0.289 g (89%) of **1b** as a colorless solid. Mp: 201–203 °C (dec). Anal. Calcd (found) for $C_{43}H_{48}N_{12}AgF_3O_7S_3$: C, 46.70 (46.81); H, 4.37 (4.72); N, 15.20 (15.31). IR (ATR, cm^{-1}): ν_{NH} 3154; triflate (s to vs), 1268 (ν_{as}, SO_3), 1224 (ν_s, CF_3), 1172 (ν_{as}, CF_3), 1032 (ν_s, SO_3), 637 (δ_s, SO_3). ^{1}H NMR (CD_3CN): δ_H 8.19 (d, *J* = 2.8 Hz, 1 H, H_{5cpz}), 7.80 (d, *J* = 8.4 Hz, 2 H, Ts), 7.46 (s, 1 H, $H_{methine}$), 7.40 (d, *J* = 8.4 Hz, 2 H, Ts), 6.12 (d, *J* = 2.8 Hz, 1 H, H_{4cpz}), 5.98 (s, 2 H, H_{4pz*}), 2.38 (s, 3H, TsMe), 2.35 (s, 6 H, pz*Me), 1.65 (s, 6H, pz*Me). ^{13}C NMR (CD_3CN): δ_C 154.81, 151.82, 147.89, 143.63, 134.59, 134.08, 131.35, 128.83, 110.53 (C_{4cpz}), 107.31 (C_{4pz*}), 65.66 ($C_{methine}$), 21.73 (TsMe), 13.63 (pz*Me), 11.36 (pz*Me). ^{19}F NMR (CD_3CN): δ_F −79.29 (s). ESI(+) MS (relative intensity) assignment: *m*/*z* 957 (6) [Ag(^{Ts}L*)$_2$]$^+$, 531 (7) [Ag(^{Ts}L*)]$^+$, 425 (9) [Ag(^{Ts}L*) – pz*]$^+$, 329 (100) [^{Ts}L* – pz]. X-ray-quality single crystals of **1b**·1.5CH_3CN were grown by vapor diffusion of Et_2O into a CH_3CN solution (1.3 mL, 0.02 M). Single crystals of **1b**·MeOH were grown by vapor diffusion of Et_2O into a MeOH solution (1.3 mL, 0.04 M).

[Ag(^{Ts}L)](OTf) (**2a**)
A mixture of 0.605 g (1.64 mmol) of ^{Ts}L and 0.422 g (1.64 mmol) of AgOTf gave 0.847 g (82%) of **2a** as a colorless solid. Mp: 141–146 °C (dec). Anal. Calcd (found) for $C_{18}H_{16}N_6AgF_3O_5S_2$: C, 34.57 (34.47); H, 2.54 (2.56); N, 13.44 (13.49). IR (ATR, cm^{-1}): tosyl, 1389 (ν_{as}, SO_2), 904 (ν_{S-N}); triflate (s to vs), 1283 (ν_{as}, SO_3), 1237 (ν_s, CF_3), 1223 (ν_s, CF_3), 1163 (ν_{as}, CF_3), 1148 (ν_{as}, CF_3), 1025 (ν_s, SO_3), 634 (δ_s, SO_3). ^{1}H NMR (CD_3CN): δ_H 8.23 (d, J = 2.8 Hz, 1 H, H_{5cpz}), 7.89 (d, J = 2.4 Hz, 2 H, H_{5pz}), 7.82 (s, 1 H, $H_{methine}$), 7.81 (d, J = 8.4 Hz, 2 H, Ts), 7.59 (d, J = 1.6 Hz, 2 H, H_{3pz}), 7.41 (d, J = 8.4 Hz, 2 H, Ts), 6.39 (dd, J = 2.4, 1.6 Hz, 2 H, H_{4pz}), 6.31 (d, J = 2.8 Hz, 1 H, H_{4cpz}), 2.41 (s, 3 H, $TsCH_3$). ^{13}C NMR (CD_3CN): δ_C 153.79, 148.10, 142.99, 134.29, 134.27, 132.68, 131.32, 128.91, 110.24 (C_{4cpz}), 107.71 (C_{4pz}), 72.03 ($C_{methine}$), 21.72 (TsMe). ^{19}F NMR (CD_3CN): δ_F −79.33 (s). ESI(+) MS (relative intensity) assignment: *m*/*z* 1101 (11) $[Ag_2(^{Ts}L)_2(OTf)]^+$, 845 (100) $[Ag(^{Ts}L)_2]^+$, 475 (87) $[Ag(^{Ts}L)]^+$, 301 (18) $[^{Ts}L - Hpz]^+$. X-ray-quality single-crystalline needles of **2a** were grown by vapor diffusion of Et_2O into a CH_3CN solution (1.25 mL, 0.03 M) over the course of 2 days. In certain cases, when vapor diffusion of more concentrated solutions (1.25 mL, 0.06 M) was prolonged over a period of 1 week, large block crystals of **2b** also formed amidst the majority of needles of **2a**.

[Ag(^{Ts}L)$_2$](OTf) (**2b**)
A mixture of 0.250 g (0.679 mmol) of ^{Ts}L and 0.0872 g (0.339 mmol) of AgOTf gave 0.251 g (77%) of **2b** as a colorless solid. Mp: 150–151 °C (dec). Anal. Calcd (found) for $C_{35}H_{32}N_{12}AgF_3O_7S_3$: C, 42.30 (41.99); H, 3.25 (3.31); N, 16.91 (16.54). IR (ATR, cm^{-1}) tosyl, 1365 (ν_{as}, SO_2), 902 (ν_{S-N}); triflate (s to vs), 1290 (ν_{as}, SO_3), 1260 (ν_s, CF_3), 1220 (ν_s, CF_3), 1174 (ν_{as}, CF_3), 1131 (ν_{as}, CF_3), 1022 (ν_s, SO_3), 638 (δ_s, SO_3). ^{1}H NMR (CD_3CN): δ_H 8.23 (d, J = 2.8 Hz, 1 H, H_{5cpz}), 7.82 (br s, 3 H, overlapping H_{5pz} + $H_{methine}$), 7.79 (d, J = 8.4 Hz, 2 H, Ts), 7.56 (br s, 2 H, H_{3pz}), 7.40 (d, J = 8.4 Hz, 2 H, Ts), 6.36 (dd, J = 2.4, 1.6 Hz, 2 H, H_{4pz}), 6.35 (d, J = 2.8 Hz, 1 H, H_{4cpz}), 2.40 (s, 3 H, $TsCH_3$). ^{13}C NMR (CD_3CN): δ_C 154.04, 148.08, 142.50, 134.29, 134.25, 132.05, 131.32, 128.92, 110.18 (C_{4cpz}), 107.67 (C_{4pz}), 72.40 ($C_{methine}$), 21.73 (TsMe). ^{19}F NMR (CD_3CN): δ_F −79.32 (s). ESI(+) MS (relative intensity) [assignment: *m*/*z* 845 (7) $[Ag(^{Ts}L)_2]^+$, 475 (16) $[Ag(^{Ts}L)]^+$, 391 (13) $[Na(^{Ts}L)]^+$, 369 (4) $[H(^{Ts}L)]^+$, 301 (100) $[^{Ts}L - Hpz]^+$. X-ray-quality single crystals were grown by vapor diffusion of Et_2O into a CH_3OH solution (1.25 mL, 0.022 M).

[Ag(^{H}L*)](OTf) (**3a**)
A mixture of 0.200 g (0.740 mmol) of ^{H}L* and 0.190 g (0.740 mmol) of AgOTf gave 0.337 g (86%) of **3a** as a colorless solid. Mp: 186–188 °C (dec). Anal. Calcd (found) for $C_{15}H_{18}N_6AgF_3O_3S$: C, 34.17 (34.20); H, 3.44 (3.37); N, 15.94 (15.81). IR (ATR, cm^{-1}): ν_{NH} 3157; triflate (s to vs), 1286 (ν_{as}, SO_3), 1222 (ν_s, CF_3), 1168 (ν_{as}, CF_3), 1028 (ν_s, SO_3), 638 (δ_s, SO_3). ^{1}H NMR (CD_3CN): δ_H 11.47 (br s, 1 H, NH), 7.63 (d, J = 2.3 Hz, 1 H, H_{5cpz}), 7.49 (s, 1 H, $H_{methine}$), 6.17 (d, J = 2.3 Hz, 1 H, H_{4cpz}), 6.01 (s, 2 H, H_{4pz*}), 2.45 (s, 6 H, CH_3pz*), 2.06 (s, 6 H, CH_3pz*). ^{13}C NMR (CD_3CN): δ_C 151.23 (br), 151.11, 143.03, 107.05 (C_{4pz*}), 106.12 (C_{4cpz}), 64.78 ($C_{methine}$), 14.03 (pz*Me), 11.38 (pz*Me). ^{19}F NMR (CD_3CN): δ_F −79.34 (s). ESI(+) MS (relative intensity) assignment: *m*/*z* 905 (29) $[Ag_2(^{H}L*)_2(OTf)]^+$, 809 (12) $[Ag_2(^{H}L*)_2OTf - Hpz*]$, 755 (9) $[Ag_2(^{H}L*)(^{H}L* - H)]^+$, 649 (100) $[Ag(^{H}L*)_2]^+$, 551 (10) $[Ag(^{H}L*)_2 - Hpz*]^+$, 418 (27)

[Ag(^{H}L*)(CH_3CN)]+, 377 (73) [Ag(^{H}L*)]$^+$. X-ray-quality single crystals were grown by vapor diffusion of Et_2O into a CH_3CN solution (1.4 mL, 0.04 M).

[Ag(^{H}L*)$_2$](OTf) (**3b**)

A mixture of 0.150 g (0.550 mmol) of ^{H}L* and 0.0713 g (0.277 mmol) of AgOTf gave 0.170 g (77%) of **3b** as a colorless solid after drying at 100 °C for 4 h under vacuum. Mp: 181–183 °C (dec). Anal. Calcd (found) for $C_{29}H_{36}N_{12}AgF_3O_3S$: C, 43.67 (44.01); H, 4.55 (4.64); N, 21.07 (21.28). IR (ATR, cm^{-1}): ν_{NH} 3375; triflate (s to vs), 1283 (ν_{as}, SO_3), 1223 (ν_s, CF_3), 1151 (ν_{as}, CF_3), 1028 (ν_s, SO_3), 636 (δ_s, SO_3). ^{1}H NMR (CD_3CN): δ_H 11.38 (br s, 1 H, NH), 7.61 (d, *J* = 2.3 Hz, 1 H, H_{5cpz}), 7.50 (s, 1 H, $H_{methine}$), 6.14 (d, *J* = 2.3 Hz, 1 H, H_{4cpz}), 6.00 (s, 2 H, H_{4pz*}), 2.45 (s, 6 H, CH_3pz*), 1.98 (s, 6 H, CH_3pz*). ^{13}C NMR (CD_3CN): δ_C 150.98, 142.74, 106.92 (C_{4pz*}), 106.00 (C_{4cpz}), 65.50 ($C_{methine}$), 13.66 (pz*Me), 11.40 (pz*Me). ^{19}F NMR (CD_3CN): δ_F −79.32 (s). ESI(+) MS (relative intensity) assignment: *m*/*z* 647 (100) [Ag(^{H}L*)$_2$]$^+$, 418 (2) [Ag(^{H}L*)(CH_3CN)]$^+$, 377 (23) [Ag(^{H}L*)]$^+$, 175 (44) [L – pz*]. A sample that was dried under vacuum but without heating analyzed as **3b**·0.5THF·0.5H_2O. Anal. Calcd (found) for $C_{31}H_{41}N_{12}AgF_3O_4S$: C, 44.19 (44.04); H, 4.90 (4.75); N, 19.95 (20.08). X-ray-quality single crystals were grown by vapor diffusion of Et_2O into a CH_3OH solution (1.3 mL, 0.02 M).

[Ag(HL)](OTf) (4a)

A mixture of 0.196 g (0.915 mmol) of ^{H}L and 0.235 g (0.915 mmol) of AgOTf gave 0.366 g (85%) of **4a** as a colorless solid. Mp: 175–178 °C (dec). Anal. Calcd (found) for $C_{11}H_{10}N_6AgF_3O_3S$: C, 28.04 (28.39); H, 2.14 (2.31); N, 17.84 (17.86). IR (ATR, cm^{-1}) ν_{NH} 3154; triflate (s to vs), 1276 (ν_{as}, SO_3), 1224 (ν_s, CF_3), 1167 (ν_{as}, CF_3), 1027 (ν_s, SO_3), 632 (δ_s, SO_3). ^{1}H NMR (CD_3CN): δ_H 11.90 (br s, 1 H, NH), 7.96 (d, *J* = 2.6 Hz, 2 H, H_{5pz}), 7.93 (s, 1 H, $H_{methine}$), 7.71 (d, *J* = 2.4 Hz, 1 H, H_{5cpz}), 7.62 (d, *J* = 1.8 Hz, 2 H, H_3pz), 6.38 (m, 3 H, overlapping $H_{4pz\&4cpz}$). ^{13}C NMR (CD_3CN): δ_C 143.42 (br), 143.09, 132.70, 131.64, 107.49 (C_{4pz}), 106.49 (C_{4cpz}), 71.70 ($C_{methine}$). ^{19}F NMR (CD_3CN): δ_F −79.29 (s). ESI(+) MS (relative intensity) assignment: *m*/*z* 1265 (3) [Ag_3(^{H}L)$_3$(OTf)$_2$]$^+$, 1051 (1) [Ag_3(^{H}L)$_2$(OTf)$_2$]$^+$, 793 (41) [Ag_2(^{H}L)$_2$(OTf)]$^+$, 678 (3) [Ag_2(^{H}L)$_2$Cl]$^+$, 643 (32) [Ag_2(^{H}L)(^{H}L – H)]$^+$, 579 (4) [Ag_2(^{H}L)(OTf)]$^+$, 535 (95) [Ag(^{H}L)$_2$]$^+$, 465 (6) [Ag_2(^{H}L)(Cl)]$^+$, 361 (35) [Ag(^{K}L)]$^+$, 323 (100) [Ag(^{H}L)]$^+$. X-ray-quality single crystals were grown by vapor diffusion of Et_2O into a CH_3CN solution (1.4 mL, 0.04 M).

[Ag(HL)2](OTf) (4b)

A mixture of 0.192 g (0.896 mmol) of ^{H}L and 0.115 g (0.448 mmol) of AgOTf in 20 mL of THF gave a solution (no precipitate) after 1 h, so the solvent was removed by vacuum distillation. The colorless residue was washed with Et_2O and dried at 100 °C under vacuum for 4 h to give 0.218 g (71%) of **4b** as a colorless solid. Mp: 124–126 °C (dec). Anal. Calcd (found) for $C_{21}H_{20}N_{12}AgF_3O_3S$: C, 36.80 (36.44); H, 2.94 (3.12); N, 24.52 (24.50). IR (ATR, cm^{-1}): ν_{NH} 3126; triflate (s to vs), 1276 (ν_{as}, SO_3), 1224 (ν_s, CF_3), 1158 (ν_{as}, CF_3), 1029 (ν_s, SO_3), 637 (δ_s, SO_3). ^{1}H NMR (CD_3CN): δ_H 11.82 (br s, 1 H, NH), 7.91 (d, *J* = 2.6 Hz, 2 H, H_{5pz}), 7.90 (s, 1 H, $H_{methine}$), 7.69 (d, *J* = 2.4 Hz, 1 H, H_{5cpz}), 7.58 (d, *J* = 1.8 Hz, 2 H, H_3pz), 6.37 (m, 3 H, overlapping $H_{4pz\&4cpz}$). ^{13}C NMR (CD_3CN): δ_C 142.62, 132.12, 131.55, 107.48 (C_{4pz}), 106.25 (C_{4cpz}), 72.45 ($C_{methine}$). ^{19}F NMR (CD_3CN): δ_F −79.31 (s). ESI(+) MS (relative intensity) assignment: *m*/*z* 535 (57) [Ag(^{H}L)$_2$]$^+$, 362 (5) [Ag(^{H}L)(CH_3CN)]$^+$, 321 (100) [Ag(^{H}L)]$^+$, 147(60) [L

– H_{pz}]. X-ray-quality single-prismatic crystals of **4b**·acetone·H_2O were obtained by evaporation of a solution of a mixture of acetone and H_2O. The crystals analyzed as **4b**·acetone·H_2O. Anal. Calcd (found) for $C_{23}H_{26}N_{12}AgF_3O_{4.5}S$: C, 37.86 (37.77); H, 3.71 (3.62); N, 22.07 (22.38). Under most other conditions (1,2-dichloroethane solutions, evaporation of THF or CH_2Cl_2 solutions, vapor diffusion of pentane into THF or acetone solutions, of Et_2O into CH_3CN or MeOH solutions, layering hexane onto acetone solutions), a mixture of mainly very long (>2 mm), highly crystalline, but extremely thin needles of **4b**·solvate was obtained along with a few plates of **4a**. After drying under vacuum at room temperature (and exposure to air), these analyzed as **4b**·solvate·H_2O. Anal. Calcd (found) for **4b**·CH_3CN·H_2O, $C_{23}H_{25}N_{13}AgF_3O_4S$: C, 37.11 (37.44); H, 3.38 (3.12); N, 24.46 (24.50).

Reactions

General Procedure for the Preparation of Tricarbonylmanganese(I) Complexes

Under an argon atmosphere and with exclusion of light (aluminum-foil-wrapped apparatus), a mixture of $Mn(CO)_5Br$ and [Ag(L)](OTf) (1 equiv) in 10 mL of CH_3CN was heated at reflux for 3 h, during which time a precipitate formed. The solution was filtered, CH_3CN was removed under vacuum, and the yellow residue was washed with two 2 mL portions of Et_2O and dried under vacuum. The yellow solids are slightly light-sensitive, so they are best stored in the dark (aluminum-foil-wrapped vials). The quantities of reagents used and of the products obtained and characterization data for each of the four new compounds are given below.

[fac-Mn(CO)3(TsL*)](OTf) (5)

A mixture of 0.127 g (0.186 mmol) of **1a** and 0.0512 g (0.186 mmol) of $Mn(CO)_5Br$ gave 0.118 g (89%) of **5** as a yellow solid. Mp: >210 °C. Anal. Calcd (found) for $C_{25}H_{24}N_6F_3MnO_8S_2$: C, 42.14 (41.97); H, 3.39 (3.43); 11.79 (11.54). IR (ATR, cm^{-1}): ν_{CO} 2038, 1931; tosyl, 1396 (ν_{as}, SO_2), 903(ν_{S-N}); triflate (CH_2Cl_2/KBr, s to vs), 1252 (ν_{as}, SO_3), 1203 (ν_s, CF_3), 1153 (ν_{as}, CF_3), 1026 (ν_s, SO_3), 630 (δ_s, SO_3). ^1H NMR (CD_3CN, 333 K, two species in a 5:1 ratio): major, δ_H 8.49 (br s, 1 H, H_{5cpz}), 7.78 (d, J = 7.5 Hz, 2 H, Ts), 7.61 (s, 1 H, $H_{methine}$), 7.43, (d, J = 7.5 Hz, 2 H, Ts), 7.17 (br s, 1 H, H_{4cpz}), 6.15 (s, 2 H, H_{4pz*}), 2.52 (s, 6 H, pz*CH_3), 2.50 (s, 6 H, pz*CH_3), 2.42 (s, 3 H, TsCH_3); minor, δ_H 7.89 (s, 1 H, $H_{methine}$), 6.90 (s, 1 H, H_{5cpz}), 6.12 (s, 2 H, H_{4pz*}), 5.42 (s, 1 H, H_{4cpz}); Ts and pz*CH_3 protons not observed, overlapping major resonances. ^{13}C NMR (CD_3CN, only resonances for major species are given): δ_C 221.30 (CO), 220.86 (CO), 157.40, 153.84, 149.33, 145.27, 142.11, 133.84, 131.76, 128.79, 111.61 (C_{4cpz}), 110.16 (C_{4pz}), 60.86 ($C_{methine}$), 21,78 (TsMe), 15.15 (pz*Me), 11.45 (pz*Me); resonance for CF_3 not observed. ^{19}F NMR (CD_3CN): δ_F −78.87 (s). ESI(+) MS (relative intensity) assignment: *m*/*z* 563 (100) $[Mn(CO)_3(^{Ts}L^*)]^+$, 497 (19) $[Mn(H_2O)(^{Ts}L^*)]$, 433 (5) $[Mn(CO)_3(^{Na}L^*)]^+$. UV–vis [CH_3CN; λ, nm (ε, M^{-1} cm^{-1})]: 359 (2430). Twinned needle crystals were grown by heating a mixture of 50 mg of **5** in 0.5 mL of MeOH to dissolution and then cooling the solution to room temperature.

[fac-Mn(CO)3(TsL)](OTf) (6)

A mixture of 0.200 g (0.320 mmol) of **2a** and 0.088 g (0.320 mmol) of $Mn(CO)_5Br$ gave 0.165 g (79%) of **6** as a yellow solid. X-ray-quality single crystals were grown by diffusion of a layer of

3 mL of hexanes into a CH_2Cl_2 solution (1.5 mL, 0.014 M) or layering 5 mL of Et_2O onto a CH_3CN solution (1.4 mL, 0.03 M). Mp: 144 °C (dec). Anal. Calcd (found) for $C_{21}H_{16}N_6F_3MnO_8S_2$: C, 38.42 (38.46); H, 2.46 (2.61); 12.80 (12.57). IR (ATR, cm^{-1}): ν_{CO} 2045, 1933; tosyl, 1396 (ν_{as}, SO_2), 910 (ν_{S-N}); triflate (s to vs), 1250 (ν_{as}, SO_3), 1159 (ν_{as}, CF_3), 1020 (ν_s, SO_3), 625 (δ_s, SO_3). ^{1}H NMR (CD_3CN, 333 K; two species in a 5:1 ratio): major species, δ_H 8.44 (d, J = 3.0 Hz, 1 H, H_{5cpz}), 8.27 (d, J = 2.8 Hz, 2 H, H_{5pz}), 8.24 (s, 1 H, $H_{methine}$), 8.21 (d, J = 2.0 Hz, 2 H, H_{3pz}), 7.80 (d, J = 8.4 Hz, 2 H, Ts), 7.44 (d, J = 8.4 Hz, 2 H, Ts), 7.06 (d, J = 3.0 Hz, 1 H, H_{4cpz}), 6.55 (dd, J = 2.8 and 2.0 Hz, 2 H, H_{4pz}), 2.42 (s, 3 H, $TsCH_3$); minor species, δ_H 8.32 (d, J = 2.8 Hz, 2 H, H_{5pz}), 8.28 (s, 1 H, $H_{methine}$), 8.15 (d, J = 2.0 Hz, 2 H, H_{3pz}), 8.14 (d, J = 2.7 Hz, 1 H, H_{5cpz}), 7.72 (d, J = 8.5 Hz, 2 H, Ts), 7.42 (d, J = 8.5 Hz, 2 H, Ts), 6.74 (dd, J = 2.8 and 2.0 Hz, 2 H, H_{4pz}), 5.85 (d, J = 2.7 Hz, 1 H, H_{4cpz}), 2.43 (s, 3 H, $TsCH_3$). ^{13}C NMR (CD_3CN): δ_C 221.29 (CO), 214.95 (CO), 149.39, 148.15, 141.19, 136.19, 131.77, 130.99, 129.56, 128.91, 111.55 (C_{4cpz}), 109.79 (C_{4pz}), 66.34 ($C_{methine}$), 21.78 (TsMe). ^{19}F NMR (CD_3CN): δ_F −79.26 (s). ESI(+) MS (relative intensity) assignment: *m*/*z* 507 (100) $[Mn(CO)_3(^{Ts}L)]^+$, 441 (29) $[Mn(H_2O)(^{Ts}L)]^+$, 423 (3) $[Mn(^{Ts}L)]^+$, 418 (5) $[Mn(CO)_3(^{Na(CH_3CN)}L)]^+$, 377 (11) $[Mn(CO)_3(^{Na}L)]^+$, 359 (4) $[Mn(CO)_3(^{Li}L)]^+$. UV–vis [CH_3CN; λ, nm (ε, M^{-1} cm^{-1})]: 353 (2430).

[fac-Mn(CO)3(HL*)](OTf) (7)

A mixture of 0.158 g (0.299 mmol) of **3a** and 0.0822 g (0.299 mmol) of $Mn(CO)_5Br$ gave 0.151 g (85%) of **7** as a yellow solid. Mp: 170 °C (dec). Anal. Calcd (found) for $C_{18}H_{18}N_6F_3MnO_6S$: C, 38.72 (38.59); H, 3.25 (3.62); 15.05 (15.01). IR (Nujol/KBr, cm^{-1}): ν_{NH} 3413. IR (ATR, cm^{-1}): ν_{CO} 2034, 1928; triflate (CH_2Cl_2/KBr, s to vs), 1276 (ν_{as}, SO_3), 1225 (ν_s, CF_3), 1157 (ν_{as}, CF_3), 1028 (ν_s, SO_3), 625 (δ_s, SO_3). ^{1}H NMR (CD_3CN): δ_H 7.89 (br s, 1 H, H_{5cpz}), 6.64 (br s, 1 H, $H_{methine}$), 6.89 (br s, 1 H, H_{4cpz}), 6.12 (br s, 2 H, H_{4pz*}), 2.51 (br s, CH_3), 2.49 (br s, CH_3); N–H not observed. ^{13}C NMR (CD_3CN): δ_C 221.52 (CO), 215.59 (CO), 156.49, 144.58, 134.96, 109.44 (C_{4pz*}), 106.49 (C_{4cpz}), 60.87 ($C_{methine}$), 15.15 (pz*Me), 11.41 (pz*Me). ^{19}F NMR (CD_3CN): δ_F −79.28 (s). ESI(+) MS (relative intensity) assignment: *m*/*z* 409 (100) $[Mn(CO)_3(^{H}L*)]^+$, 366 (11) $[Mn(CH_3CN)(^{H}L*)]^+$, 353 (21) $[Mn(CO)(^{H}L*)]^+$, 325 (43) $[Mn(^{H}L*)]^+$. UV–vis [CH_3CN; λ, nm (ε, M^{-1} cm^{-1})]: 347 (2360). Crystals can be obtained by diffusion of a layer of 5 mL of Et_2O into a CH_3CN solution (1.4 mL, 0.03 M).

[fac-Mn(CO)3(HL)](OTf) (8)

A mixture of 0.200 g (0.425 mmol) of **4a** and 0.117 g (0.425 mmol) of $Mn(CO)_5Br$ gave 0.187 g (88%) of **8** as a yellow solid. Mp: >210 °C. Anal. Calcd (found) for $C_{14}H_{10}N_6F_3MnO_6S$: C, 33.09 (33.31); H, 1.98 (2.03); N, 16.54 (16.44). IR (Nujol/KBr, cm^{-1}): ν_{NH} 3396. IR (ATR, cm^{-1}): ν_{CO} 2043, 1944; triflate (CH_2Cl_2/KBr, s to vs), 1288 (ν_{as}, SO_3), 1221 (ν_s, CF_3), 1145 (ν_{as}, CF_3), 1018 (ν_s, SO_3), 619 (δ_s, SO_3). ^{1}H NMR (CD_3CN, 333 K): δ_H 12.85 (br s, N–H), 8.22 (br s, 2H, H_{3pz}), 8.18 (d, J = 2 Hz, 2 H, H_{5pz}), 8.14 (br s, $H_{methine}$), 7.87 (br s, 1 H, H_{5cpz}), 6.81 (br s, 1 H, H_{4cpz}), 6.49 (br m, 2 H, H_{4pz}). ^{13}C NMR (CD_3CN, 295 K): δ_C 221.29 (CO), 213.17 (CO), 147.67, 145.38, 135.50, 134.64, 109.13 (C_{4cpz}), 106.87 (C_{4pz}), 66.71 ($C_{methine}$); CF_3 resonances not observed. ^{19}F NMR (CD_3CN): δ_F −79.24 (s). ESI(+) MS (relative intensity) assignment: *m*/*z* 353 (96) $[Mn(CO)_3(^{H}L)]^+$, 310 (48) $[Mn(CH_3CN)(^{H}L)]^+$, 287 (11) $[Mn(CO)_3(^{H}L*) - pz]^+$, 269 (100)

[Mn(^{H}L)]$^{+}$. UV–vis [CH_3CN; λ, nm (ε, M^{-1} cm^{-1})]: 346 (2300). X-ray-quality single crystals were grown by diffusion of a layer of 3 mL of hexanes into a CH_2Cl_2 solution (1.9 mL, 0.04 M).

[Fe(HL)2](OTf)2 (9)

Method A. A solution of 0.250 g (1.17 mmol) of ^{H}L in 10 mL of THF was added to a solution of 0.207 g (0.585 mmol) of $Fe(OTf)_2$ in THF under argon. A yellow-orange solid initially precipitated but changed pink within 30 min. After the resulting pink suspension had been stirred for 16 h, THF was removed by cannula filtration and the solid was washed with 5 mL of Et_2O then dried in a 140 °C oven for 2 h to give 0.341 g (75%) of **9** as a pink powder. Purple single crystals suitable for X-ray diffraction were grown by vapor diffusion of Et_2O into a solution of 15 mg of **9** in 1.5 mL of MeOH. Characterization data listed below are for crystals or dissolved crystals.

Method B. A solution of 0.205 g (0.434 mmol) of **4a** in 10 mL of MeOH was added to an argon-purged solution of 0.0275 g (0.217 mmol) of $FeCl_2$ in 10 mL of H_2O. Upon mixing, a purple solution and colorless precipitate formed. After the mixture had been stirred for 45 min, the precipitated AgCl was removed by filtration and solvent was removed from the filtrate under vacuum to leave 0.150 g (89%) of **9** as a pink-purple powder.

Method C. A mixture of 0.0500 g (0.106 mmol) of **4a** and 0.0030 g (0.053 mmol) of Fe^0 powder in 8 mL of CH_3CN was heated at reflux for 14 h with vigorous stirring. The resulting pink solution was separated from the metallic residue by cannula filtration. The residue was washed with two 2 mL portions of CH_3CN. After removing the solvent from the combined CH_3CN soluble fractions by vacuum distillation, a purple solid remained. The solid was dissolved in 1 mL of MeOH, and the solution was subjected to Et_2O vapor diffusion over 2 days. The mother liquor was decanted from the so-formed red-purple crystals. The crystals were washed with Et_2O and were dried under vacuum for 30 min to give 0.028 g (53%) of **9** as red-purple crystals.

Characterization Data for 9

Mp: colorless by 110 °C; did not melt below 250 °C. Anal. Calcd (found) for $C_{22}H_{20}N_{12}F_6FeO_6S_2$: C, 33.77 (34.05); H, 2.58 (2.71); 21.48 (21.40). μ_{eff} (Evan's, CD_3OD): 2.0 μ_B. IR (Nujol/KBr, cm^{-1}): ν_{NH} 3140; triflate (CH_2Cl_2/KBr, s to vs), 1265 (ν_{as}, SO_3), 1232 (ν_s, CF_3), 1164 (ν_{as}, CF_3), 1018 (ν_s, SO_3), 623 (δ_s, SO_3). UV–vis [CH_3CN; λ, nm (ε, M^{-1} cm^{-1})]: 214 (25700), 271 (4650), 315 (sh, 6200), 331 (7300), 520 (100), 1103 (6). ^{1}H NMR ($CDCl_3$): δ_H 46.21, 30.71, 23.33, 20.19, 11.56, 7.17, −9.96. ESI(+) MS (relative intensity) assignment: *m*/*z* 633 (1) [Fe(^{H}L)$_2$(OTf)]$^{+}$, 483 (10) [Fe(^{H}L)(L)]$^{+}$, 243 (8) [Fe(^{H}L)$_2$]$^{2+}$, 209 (9) [Fe(^{H}L)(HL – pz)]$^{2+}$, 177 (15) [Fe(^{H}L)(CH_3CN)$_2$]$^{2+}$, 156 (11) [Fe(^{H}L)(CH_3CN)]$^{2+}$, 147 (100) [^{H}L – pz]$^{+}$. If crystals were dried under vacuum for 30 min but not heated at 140 °C for 2 h, then the sample repeatedly analyzed as **9**·MeOH: Anal. Calcd (found) for $C_{23}H_{24}N_{12}F_6FeO_7S_2$: C, 33.92 (33.86); H, 2.97 (2.69); 20.64 (20.65).

Catalytic Aziridination

To ensure reproducibility, AgOTf and other silver(I) complexes to be used as catalysts were dried at 100 °C under vacuum for 2 h prior to use.

General Procedure

A 0.5 g sample of activated 4 Å molecular sieves and a Teflon-coated magnetic stir bar were added to a Schlenk flask under an argon blanket. The flask was flame-dried under vacuum, then backfilled with argon, and allowed to cool to room temperature. Next, the silver catalyst (0.020 mmol), 0.171 g (1.00 mmol) of tosylamine, and 0.322 g (1.00 mmol) of $PhI(OAc)_2$ were added under an argon blanket. The reaction flask was subjected to three evacuation and argon backfill cycles. Next, 4 mL of dry distilled CH_3CN was added by syringe. The reaction flask was placed in an oil bath maintained at 80 °C and allowed to equilibrate for 15 min. Then, 0.57 mL (0.521 g, 5.00 mmol) of styrene was added by syringe, at which time the solution changed color to orange or, in some instances, orange-brown. After the reaction mixture had been stirred at 80 °C for 16 h, it was filtered through a sintered glass frit. The solid residue was washed with two 2 mL portions of CH_3CN. Next, between 25 and 30 mg of bis(trimethylsilyl)benzene was added to the solvate as a nonvolatile NMR standard, and solvent was removed by rotary evaporation to leave a brown-orange oily residue. The residue was separated by column chromatography on silica gel by first flushing with hexanes to remove the first fraction (which moves with the solvent front) that contains the NMR standard and iodobenzene. The eluent was then changed to 4:1 (v/v) hexanes/EtOAc. The next (second) fraction (R_f = 0.7) was a diastereomeric mixture of 2,4-diphenyl-*N*-tosylpyrrolidine,[(36)] and the third fraction ($R_f \sim 0.4$) contained the desired aziridine. The excess H_2NTs and an unidentified brown product remained in the column (but could be eluted with MeOH if desired). The yields of aziridine are the average of a minimum of three catalytic runs.

Crystallography

X-ray intensity data from a colorless needle of **1a**, a colorless plate of **1b**, a colorless prism of **1b**·MeOH, a colorless needle of **2a**, a colorless irregular block of **2b**, a colorless prism of **3a**, a colorless plate of **3b**, a colorless plate of **4a**, a yellow plate of **6**, a yellow prism of **8**, and a pink prism of **9** were each collected at 100.0(1) K with an Oxford Diffraction Ltd. A Supernova diffractometer equipped with a 135 mm Atlas CCD detector using Cu Kα radiation for the data of **1a**, **1b**·1.5CH_3CN, **1b**·CH_3OH, **3b**, **4b**·acetone·H_2O, **8**, and **9** was used, while Mo Ka radiation was used for the other experiments. Raw data frame integration and Lp corrections were performed with *CrysAlisPro* (Oxford Diffraction, Ltd.).[(37)] Final unit cell parameters were determined by least-squares refinement of the 15713, 22719, 14418, 10710, 25334, 19082, 19683, 14285, 18698, 27362, 6891, and 6853 reflections of **1a**, **1b**·1.5CH_3CN, **1b**·MeOH, **2a**, **2b**, **3a**, **3b**, **4a**, **4b**·acetone·H_2O, **6**, **8**, and **9**, respectively, with $I > 2\sigma(I)$ for each. Analysis of the data showed negligible crystal decay during collection in each case. Direct-method structure solutions were performed with *Olex2.solve*,[(38)] while difference Fourier calculations and full-matrix least-squares refinements against F^2 were performed with *SHELXTL*.[(39)] Numerical absorption corrections based on Gaussian integration over a multifaceted crystal model were applied to the data for each of the complexes except for **9**, which employed a multiscan empirical absorption correction using spherical harmonics, as implemented in the *SCALE3 ABSPACK* scaling algorithm. All non-hydrogen atoms were refined with anisotropic displacement parameters. Hydrogen atoms bond to nitrogen atoms in the structures **3a**, **3b**, **4a**, **4b**·acetone·H_2O, **8**, and **9** were located and refined, whereas all other hydrogen atoms

were placed in geometrically idealized positions and included as riding atoms. The X-ray crystallographic parameters and further details of data collection and structure refinements are given in Tables S1–S3. *Special details:* The crystal of **3b** was a nonregular twin with a 2:1 component ratio, where component 2 was rotated by 5.441° around [0.59 0.68 0.43] in reciprocal space. The structure of **4a** shows polymeric chains along *z* that possess strong quasi-symmetry: a 2-fold axis through ions Ag1 and Ag2 results in a higher centrosymmetric pseudosymmetry of the crystal, *P*2/*c*. However, an attempt at refinement in the centrosymmetric space group resulted in a much higher *R* ∼ 13%, whereas refinement as a racemic twin (with a 31:69 component ratio) in space group *Pc* gave *R* = 6.8% [Flack parameter, 0.00(16)]. Therefore, the noncentrosymmetric model was chosen. The crystal of **4b**·acetone·H_2O was a nonregular twin with a 2:1 component ratio and a 2.38° rotation around [−0.97 0.18 0.16] (reciprocal space). The structure of **9** represents a regular quasi-merohedral (pseudoorthogonal) twin (rotation 180° around *x*) with a 61:39 component ratio.

Results and Discussion

The new nitrogen-confused scorpionate ligands, ^{Ts}L* and ^{H}L*, each with two 3,5-dimethylpyrazolyl groups and either an *N*-tosyl or a N–H moiety, respectively, were prepared in a manner similar to that reported[31] for the parent ligands (with two unsubstituted pyrazol-1-yl groups), as summarized in Scheme 1. That is, the $CoCl_2$-catalyzed Peterson rearrangement[40] between *N*-tosyl-3-carboxaldehydepyrazole and an excess of bis(3,5-dimethylpyrazol-1-yl)carbonyl in toluene gave the desired ligand, ^{Ts}L*, in high yield. Excess O═C(pz*)$_2$ is required for high yield because the reaction with only 1 equiv consistently gave 63(±2)% yield after purification. The alternative use of O═S(pz*)$_2$ in THF (like that used in the synthesis of ^{Ts}L) in place of O═C(pz*)$_2$ in toluene gave lower yields (ca. 60%), presumably due to steric issues that required higher reaction temperature. Deprotection of ^{Ts}L* by aqueous base proceeded smoothly to give ^{H}L* but required longer reaction time than deprotection of ^{Ts}L (45 min versus 10 min), as indicated by thin-layer-chromatography monitoring. In contrast to the parent deprotected ligand, ^{H}L, which required extensive extraction, ^{H}L* is much less soluble in H_2O, so extraction and subsequent purification were uncomplicated. The *N*-tosyl ligands give characteristic IR bands near 1380 and 1180 cm^{-1} for antisymmetric and symmetric S–O stretches, respectively. The IR spectra for ^{H}L and ^{H}L* show weak bands for N–H stretches at 3430 and 3450 cm^{-1}, respectively.[41] For these latter ligands in CD_3CN, the ^{1}H NMR resonance for the N–H group appears as a broad singlet downfield near 11.3 ppm, a region similar to that found for other pyrazoles.

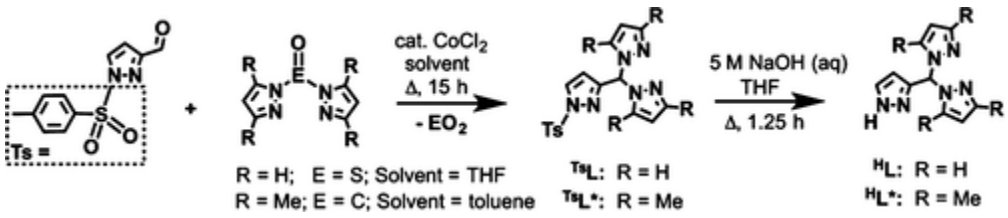

Scheme 1. Preparative Routes to Nitrogen-Confused Scorpionate Ligands

With the four ligands in hand, their 1:1 (Scheme 2) and 2:1 (Scheme 3) L/Ag(OTf) complexes were prepared in high yields by mixing THF solutions of the appropriate ligand (1 or 2 mol equiv) and 1 equiv of the silver salt and collecting the precipitate by filtration. All of the silver complexes are light-stable colorless solids. Most are air-stable, but **3b** and **4b** readily absorb adventitious H_2O, so care must be taken if one wants anhydrous complexes. Each complex is soluble in many Lewis basic organic solvents, with the exception of Et_2O (insoluble) or THF (slightly soluble), and has modest solubility in $CHCl_3$ or CH_2Cl_2. Vapor diffusion of Et_2O into either CH_3CN or CH_3OH solutions of the various complexes afforded X-ray-quality single crystals in most cases except for **4b**, for which evaporation from acetone/H_2O mixtures gave the mixed solvate.

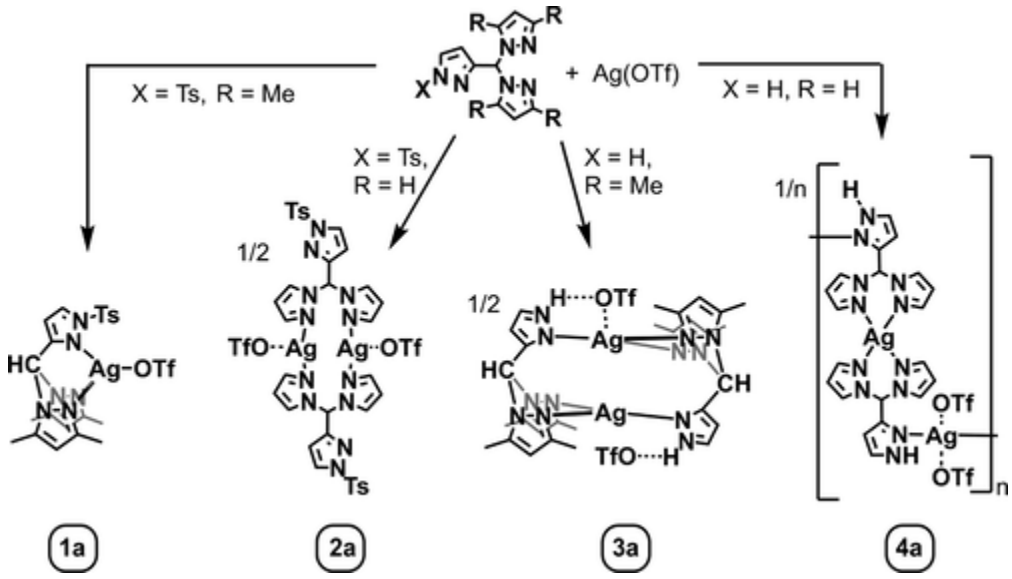

Scheme 2. Summary of the Solid-State Coordination Behavior of 1:1 ^{x}L/Ag(OTf) Complexes

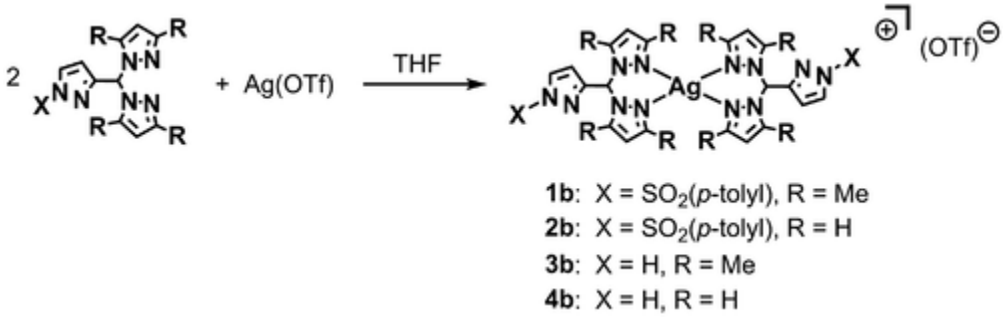

Scheme 3. Preparation and Labeling of 2:1 ^{x}L/Ag(OTf) Complexes

Solid State

Views of the structures of the various silver complexes are provided in Figures 2–7 and S1–S12. More complete details of the supramolecular structures that show three-dimensional organization by weak charge-assisted hydrogen bonding between the triflate anion and acidic hydrogen atoms of the cations in each compound are given in the Supporting Information.

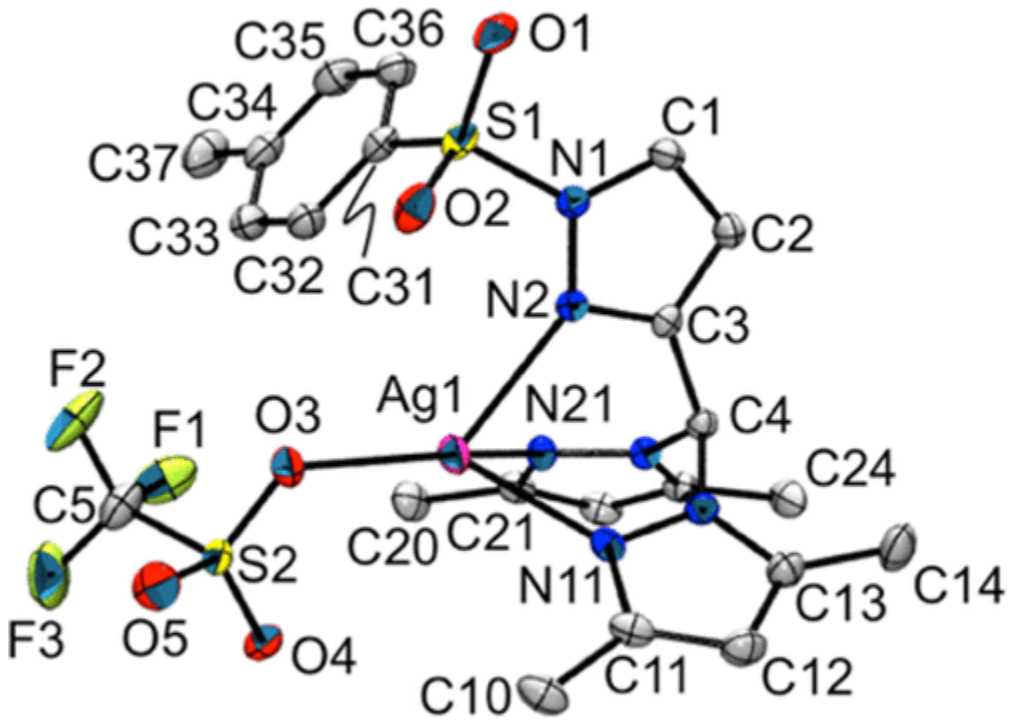

Figure 2. Structure of **1a** with hydrogen atoms removed for clarity.

As illustrated in Figure 2, **1a** features four-coordinate silver as a result of binding to the tridentate, κ^3N, ligand and a triflate oxygen. Noteworthy is the fact that while the Ag–N bond of tosylpyrazolyl is nearly 0.1 Å longer than those of the other pyrazolyls (Table 1), the average Ag–N_{pz} distance of 2.37 Å is firmly in the 2.3–2.4 Å range for other four-coordinate silver pyrazolyl complexes[42] including {[κ^3-(3-tBupz)$_3$CH]Ag}(OTf) (avg 2.38 Å)[22a] and {[κ^3-(3-Phpz)$_3$CH]Ag(CH_3CN)})BF_4 (2.36 Å).[22b] The three pyrazolyls are also disparately twisted, as quantified by either the Ag–N–C–C_{meth} torsion angle of the "confused" pyrazolyl (4°, here) or the Ag–N–N–$C_{methine}$ torsion angles of the "normal" pyrazolyls (6 and 18° for rings containing N11 and N21, respectively). The Ag–O distance [Ag–O3 2.224(2) Å] is among the shortest known for silver triflate complexes; it is shorter than relatives such as {Ag[$C_6H_5CH_2OCH_2Cpz_3$]}OTf (2.343 Å),[43] [Ag(4-MeO-2,6-pz*$_2$-triazine)]OTf (2.292 Å),[44] and Ag[HC(pz^{3tBu})$_3$]}OTf (2.264 Å)[22a] and is between the distances found in {Ag_2(μ_2-4,13-dibenzyl-4,13-diaza-18-crown-6)}$(OTf)_2$ [2.252(3) and 2.215(3) Å].[45] The bond angles about silver in **1a** give a τ_δ parameter[46] of 0.61 near the border of a distorted sawhorse coordination geometry (τ_δ = 0.63–0.45) and a distorted tetrahedral geometry (τ_δ = ~0.9–0.63).

Table 1. Selected Bond Distances (Å) and Angles (deg) in **1a**, **2a**, and **3a**

1a		**2a**				**3a**		
Bond Distances (Å)								
Ag1–N2	2.4273(17)	Ag1–N11	2.182(2)	Ag1–O1	2.724(3)	Ag2–N32	2.173 (2)	
Ag1–N11	2.3391(18)	Ag1–N21	2.232(2)	Ag1–N2	2.196(2)	Ag2–N11	2.316(3)	
Ag1–N21	2.3434(18)	Ag1–O3	2.5864(18)	Ag1–N41	2.307(3)	Ag2–N21	2.274(3)	

1a		2a		3a			
Ag1–O3	2.2235(16)	Ag1···Ag1′	3.0588(4)	Ag1–N51	2.331(2)	Ag1···Ag2	2.8271(4)
			Bond Angles (deg)				
O3–Ag1–N11	131.19(6)	N11–Ag1–O3	95.24(7)	O1–Ag1–N41	100.53(8)	N11–Ag2–N32	136.66(9)
O3–Ag1–N21	138.16(7)	N21–Ag1–O3	85.92(7)	O1–Ag1–N51	85.39(9)	N21–Ag2–N32	138.86(9)
N2–Ag1–N11	80.90(6)			N2–Ag1–N41	135.99(9)		
N2–Ag1–N21	77.27(6)			N2–Ag1–N51	141.51(9)		
O3–Ag1–N2	127.21(6)	N11–Ag1–N21	154.09(8)	O1–Ag1–N2	96.08(9)	N11–Ag2–N21	82.83(9)
N11–Ag1–N21	80.61(6)			N41–Ag1–N51	80.63(9)		

Complex **2a** exists as a dimer with inversion symmetry as a result of two ligands that sandwich two closely spaced silver centers [Ag···Ag separation 3.0588(4) Å; Figure 3]. The μ–κ^1,κ^1 ligands act in a manner where the two "normal" pyrazolyls on each ligand bind to two different silver centers with Ag–N11 of 2.182(2) Å and Ag–N21 of 2.232(2) Å. The average Ag–N distance of 2.207 Å is much longer than the 2.10–2.14 Å range found for two-coordinate silver bound to pyrazolyls[(42)] and is at the lower end of the 2.2–2.3 Å range for three-coordinate silver. The tosyl-protected "confused" pyrazolyl is highly twisted ("pz twist" = 76°) such that the very long Ag–N2 distance of 2.672 Å is probably better described as an Ag−π secondary interaction rather than a σ-bonding interaction. As a comparison, the "pz twists" of the "normal" pyrazolyls (here, with shorter Ag–N bonds) are 19° for the ring with N21 and 55° for the ring with N11. Instead, the coordination sphere about each silver center is completed by interaction with an oxygen atom of a triflate anion, Ag···O3 = 2.586(2) Å, which is within the ca. 2.07–2.75 Å range (average Ag···O distance = 2.48 ± 0.13 Å) found for other complexes of silver triflate.[(47)]

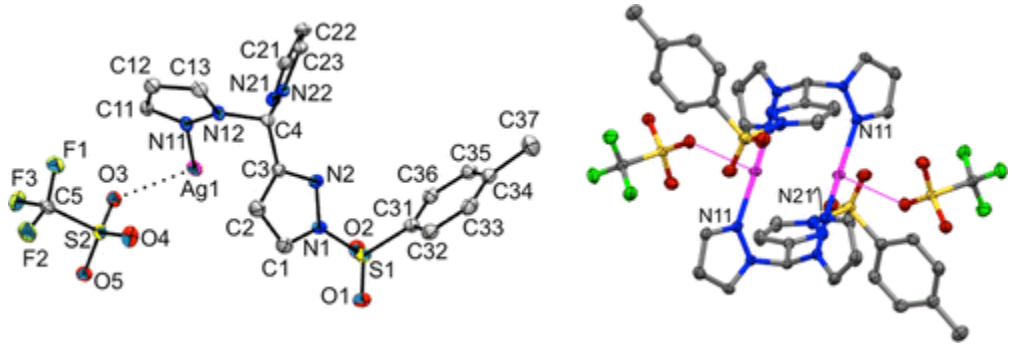

Figure 3. Views of the structure of **2a** with hydrogen atoms removed for clarity: (left) asymmetric unit with atom labeling; (right) dimeric unit.

Figure 4 shows the dimeric structure of **3a**, while Table 1 gives selected interatomic distances and angles. As opposed to dimeric **2a**, which had μ–κ^1,κ^1 ligands with an unbound "confused" pyrazolyl, the dimer in **3a** is constructed of two bridging μ–κ^2,κ^1 ligands sandwiching two silver atoms. Here, the two dimethylpyrazolyl rings chelate one silver center, while the confused pyrazolyl binds the second proximal silver to give a short Ag···Ag separation of 2.8271(4) Å

(compared to twice the van der Waals radii of silver = 3.44 Å). The ligands are arranged such that each silver is bound to one “confused” pz nitrogen and to two pz* nitrogen atoms.

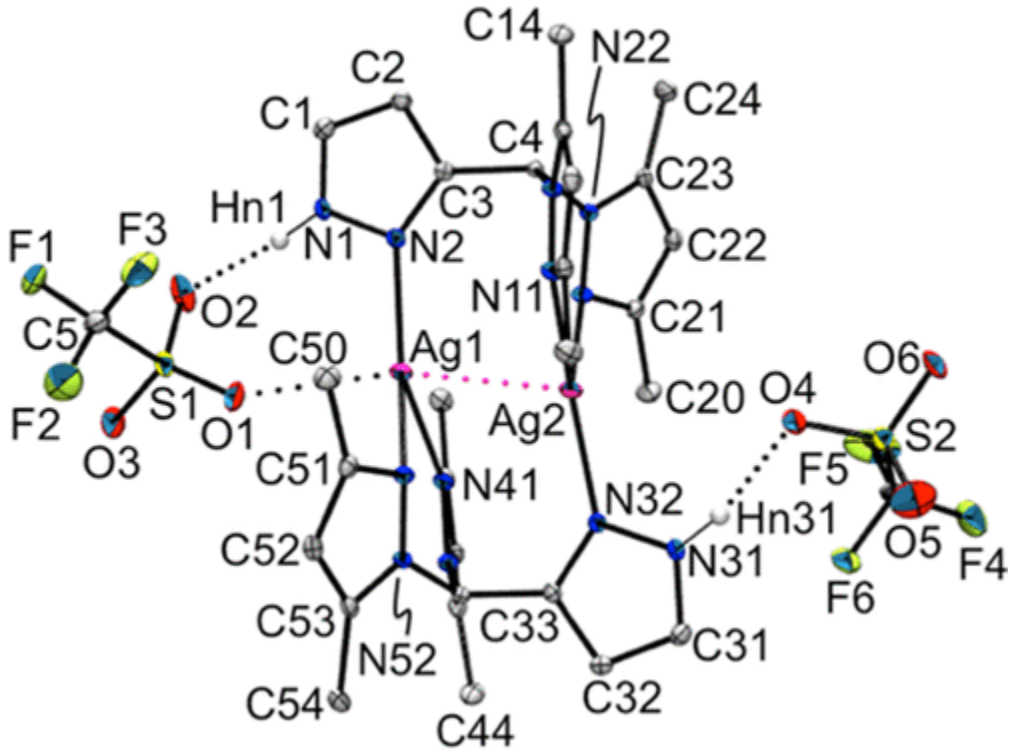

Figure 4. Structure of **3a** with partial atom labeling. Most of the hydrogen atoms are omitted for clarity.

Two triflate anions are also affixed to the dimer by short hydrogen bonds involving the confused pyrazolyl’s N–H groups (N1–H1n···O2 = 1.935 Å; N31–H31n···O4 = 1.897 Å). The triflate anion with O1 also forms a long bond with silver (Ag1–O1 = 2.724 Å), but the other triflate is not bound; the closest contact to Ag2 is with O4 at 3.632 Å. The disparity in the anion binding sites is responsible for the longer average Ag–N distance involving Ag1 (2.278 Å) than Ag2 (2.254 Å), distances that straddle the borderline demarcating three- or four-coordinate silver pyrazolyl complexes.

Complex **4a** crystallizes as a one-dimensional coordination polymer that propagates along the *c* axis as a result of bridging ligands that bind neighboring silver centers (Figure 5). The ligands show a μ–κ^2,κ^1N binding mode, where the chelating portion of the ligand is composed of the “normal” pyrazolyls, while the unidentate portion involves the “confused” pyrazolyl. These ligands are arranged so as to alternate AgN_4 and AgN_2 kernels (i.e., one silver is bound to the chelating portions of two ligands, while the other silver is bound to two κ^1N-“confused” pyrazolyl nitrogen atoms). Selected bond distances and angles are given in Table 2. The average Ag–N distances of 2.299 and 2.321 Å for Ag3 and Ag4, respectively, are clearly indicative of four-coordinate silver, whereas those of 2.153 Å for Ag1 and 2.162 Å for Ag2 are between the ranges usually found for two- and three-coordinate silver pyrazolyls. Inspection of the coordination sphere about silver reveals two long Ag–O interactions on each silver center: one that is below the 2.75 Å Ag–O bonding limit (Ag1–O7 = 2.734 Å and Ag2–O4 = 2.719 Å)

and one that is just above the limit (Ag1–O10 = 2.756 Å and Ag2–O1 = 2.767 Å). If the longer Ag–O distance were considered a secondary contact, then Ag1 and Ag2 would both be three-coordinate. Then, because Ag1 sits 0.084 Å out of the O7–N2–N2a plane, the four atoms form an acute triclinic pyramid (based on a 3% folded T), while the planar Ag2–N2b–N2c–O4 unit represents a slightly distorted T-shape (or, more specifically, a γ-constricted near-closed Y).[(48)] The “confused” pyrazolyl’s N–H group serves as a hydrogen-bond donor to triflate oxygen atoms to further secure triflate ions to the chain and between chains to assemble the supramolecular structure (Figure S8).

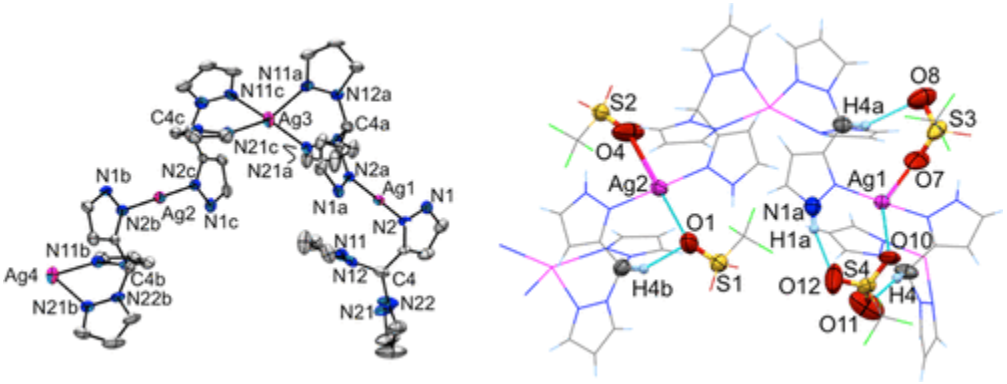

Figure 5. Portion of the structure of **4a** with partial atom labeling. Most hydrogen atoms are removed for clarity, and thermal ellipsoids are shown at 30% probability.

Table 2. Selected Bond Distances (Å) and Angles (deg) in **4a**

Bond Distances (Å)			
Ag1–N2	2.158(8)	Ag2–N2b	2.176(8)
Ag1–N2a	2.150(8)	Ag2–N2c	2.148(8)
Ag3–N11a	2.322(10)	Ag4–N11	2.266(10)
Ag3–N11c	2.339(10)	Ag4–N21	2.365(12)
Ag3–N21a	2.275(9)	Ag4–N11b	2.282(8)
Ag3–N21c	2.258(9)	Ag4–N21b	2.370(9)

Bond Angles (deg)			
N2–Ag1–N2a	175.3(3)	N2b–Ag2–N2c	179.0(3)
N11a–Ag3–N11c	113.0(3)	N11–Ag4–N11b	138.3(4)
N11a–Ag3–N21a	86.6(4)	N11–Ag4–N21	84.5(4)
N11a–Ag3–N21c	121.7(4)	N11–Ag4–N21b	124.3(4)
N11c–Ag3–N21a	123.7(4)	N11b–Ag4–N21	120.2(4)
N11c–Ag3–N21c	83.9(4)	N11b–Ag4–N21b	81.7(3)
N21a–Ag3–N21c	130.9(3)	N21–Ag4–N21b	109.1(4)

The structures of the diligated [Ag(^{x}L)$_2$](OTf)·*n*(solvate) complexes, **1b**·1.5CH_3CN, **1b**·CH_3OH, **2b**, **3b**, and **4b**·acetone·H_2O (Scheme 3), were determined, and those of the latter two complexes are given in Figures 6 and 7, while the others are provided in the Supporting

Information. Selected bond distances and angles in four of the five complexes are summarized in Table 3; the data for **1b**·CH_3OH are nearly identical with those of the acetonitrile solvate, so they are given in the Supporting Information. Each has four-coordinate silver as a result of the metal binding to the nitrogen atoms of the "normal" pyrazolyl rings; the "confused" pyrazolyl ring of each ligand is not bound to the metal center. The average Ag–N distances are quite similar across the series and are in the expected range for four-coordinate silver(I) pyrazolyl complexes: 2.33 Å in each solvate of **1b**, 2.31 Å in **2b**, 2.34 Å in **3b**, 2.35 (Ag1) and 2.36 Å (Ag1a) in the two symmetry-independent units of **4b**·acetone·H_2O. The shapes of the AgN_4 coordination polyhedra are also similar, as can be gleaned from examination of their bond angles and associated τ_δ values: τ_δ = 0.56 for both solvates of **1b** and for **3b**, τ_δ = 0.71 for **2b**, and τ_δ = 0.63 (Ag1) or 0.59 (Ag1a) for the independent units in **4b**·acetone·H_2O. All of these values are within the ranges for either a distorted tetrahedral (τ_δ = ∼0.90–0.63) or a distorted sawhorse (τ_δ = ∼0.63–0.45) geometry.[(46)] The unbound "confused" pyrazolyls in each complex involve disparate noncovalent interactions that help to differentiate the supramolecular structures. The SO groups of the tosyl unit in each solvate of **1b** (rather than of the triflate) are hydrogen-bonded to the methine hydrogen atoms of the neighboring cations to help to organize the three-dimensional extended structure (Figures S2 and S3). In contrast, the low steric profile of the normal pyrazolyls in **2b** allows contact between the triflate anion and the acidic methine hydrogen atom and relegates the tosyl SO groups to associate with acidic pyrazolyl ring hydrogen atoms in the assembly of the three-dimensional supramolecular structure (Figure S4). The two "confused" pyrazolyl arms in **3b** are involved in different hydrogen-bonding interactions (right of Figure 6). First, one "confused" pyrazolyl acts as a hydrogen-bond donor to a triflate oxygen acceptor (N1–H1n···O1, 2.088 Å, 153°). The second "confused" pyrazolyl acts as a hydrogen-bond donor to a nitrogen atom (N1a–H1na···N2′, 1.984 Å, 168°) of the triflate-bonded confused pyrazolyl ring on a neighboring complex to form a hydrogen-bonded dimer (Figure 6, right). Such an interaction positions the triflate ion in close van der Waals contact with the pz* ring hydrogen atom and one of the methyl hydrogen atoms on the neighboring complex (C12–H12···O2, 2.793 Å, 140°; C10–H10b···O1, 2.788 Å, 143°), further securing the dimer. The "confused" pyrazolyls in **4b**·acetone·H_2O participate in hydrogen-bonding interactions with analogous rings on a neighboring cation to give a C_2-symmetric dimer (right of Figure 7). The triflate ions are hydrogen-bonded to the methine hydrogen atoms on one cation with Ag1 (C4–H4···O2, 2.215 Å, 162°), while the acetone solvate is weakly hydrogen-bonded to the methine hydrogen atoms on the other cation (C4a–H4a···O4, 2.411 Å, 147°). The solvate H_2O serves as a hydrogen-bond donor to a triflate oxygen atom on one dimer (O5–H5b···O1 2.001 Å, 171°) and the acetone oxygen atom (O5–H5a···O4, 2.133 Å, 152°) of an adjacent dimer to help organize the three-dimensional supramolecular structure (Figure S9).

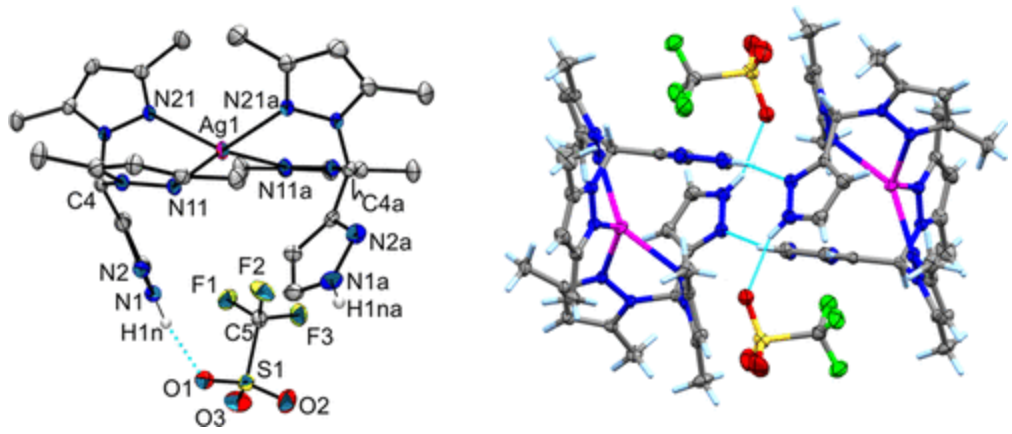

Figure 6. Views of **3b** with most of the hydrogen atoms removed for clarity and with partial atom labeling: (left) asymmetric unit; (right) hydrogen-bonded (cyan lines) dimer.

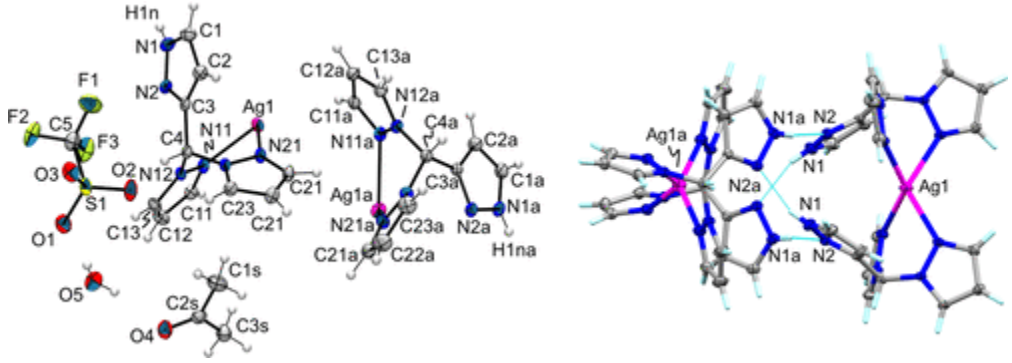

Figure 7. Structure of **4b**·acetone·H_2O: (left) asymmetric unit with atom labeling; (right) hydrogen-bonded (cyan lines) dimer of cations.

Table 3. Selected Bond Distances (Å) and Angles (deg) in **1b**·1.5CH_3CN, **2b**, **3b**, and **4b**·acetone·H_2O

1b·1.5CH_3CN		**2b**		**3b**		**4b·acetone·H_2O**			
Bond Distances (Å)									
Ag1–N11	2.339(2)	Ag1–N11	2.3066(13)	Ag1–N11	2.3839(19)	Ag1–N11	2.293(2)	Ag1a–N11a	2.465 (2)
Ag1–N21	2.318(2)	Ag1–N11a	2.3705(13)	Ag1–N21	2.3067(19)	Ag1–N21	2.412(2)	Ag1a–N21a	2.248 (2)
Ag1–N11a	2.315(2)	Ag1–N21	2.3002(12)	Ag1–N11a	2.3218(19)				
Ag1–N21a	2.332(2)	Ag1–N21a	2.2749(12)	Ag1–N21a	2.3387(19)				
Bond Angles (deg)									
N11–Ag1–N21	79.42(7)	N11–Ag1–N11a	130.14(4)	N11–Ag1–N21	83.42(6)	N11–Ag1–N11′	137.56(9)	N11a-Ag1a-N11a′	125.30(8)

1b·1.5CH_3CN		**2b**		**3b**		**4b·acetone·H_2O**			
N11–Ag1–N11a	143.21(7)	N11–Ag1–N21	85.02(4)	N11–Ag1–N11a	143.43(7)	N11–Ag1–N21	80.69(6)	N11a–Ag1a–N21a	85.14(6)
N11–Ag1–N21a	111.72(8)	N21–Ag1–N11a	109.33(4)	N21–Ag1–N21a	125.16(6)	N11–Ag1–N21′	121.15(7)	N11a–Ag1a–N21a′	113.16(6)
N21–Ag1–N11a	119.94(7)	N11–Ag1–N21a	127.92(4)	N11a–Ag1–N21	126.25(6)	N11′–Ag1–N21′	80.69(6)	N11a′–Ag1a–N21a′	85.14(6)
N21–Ag1–N21a	130.92(7)	N21–Ag1–N21a	125.98(5)	N21–Ag1–N11a	100.52(6)	N11′–Ag1–N21	121.15(7)	N11a′–Ag1a–N21a	113.16(6)
N11a–Ag1–N21a	80.30(7)	N11a–Ag1–N21a	82.44(4)	N11a–Ag1–N21a	80.31(7)	N21–Ag1–N21′	121.17(8)	N21a–Ag1a–N21a′	140.77(10)

Solution

The nature of silver(I) complexes in an acetonitrile solution was investigated intensively by spectroscopic methods (one-dimensional and diffusion NMR and IR) and by ESI(+) MS because this solvent is used for the catalytic reactions described later. The collective data indicate that all have dynamic solution structures where the static solid-state structures are not retained. Instead, it is likely that the complexes are dissociated and that multiple species exist in solution as a result of two or more of the following equilibria (eqs 1–4).

$$\frac{1}{n}[\mathrm{Ag(L)}]_n(\mathrm{OTf})_n \leftrightarrows [\mathrm{Ag(L)}](\mathrm{OTf}) \quad (1)$$

$$[\mathrm{Ag(L)}](\mathrm{OTf}) \leftrightarrows \mathrm{Ag(OTf)} + \mathrm{L} \quad (2)$$

$$[\mathrm{Ag(L)}](\mathrm{OTf}) + \mathrm{L} \leftrightarrows [\mathrm{Ag(L)_2}](\mathrm{OTf}) \quad (3)$$

$$[\mathrm{Ag(L)}](\mathrm{OTf}) \leftrightarrows \frac{1}{2}[\mathrm{Ag(L)_2}](\mathrm{OTf}) + \frac{1}{2}\mathrm{Ag(OTf)} \quad (4)$$

The equilibria are demonstrated by multiple different observations. First, crystallizations of analytically pure samples of [AgL](OTf) in either CH_3CN or CH_3OH produce mixtures of crystals. Vapor diffusion of dilute solutions (0.005 M) gives mainly the monoligated silver along with small amounts of the diligated [AgL_2](OTf), whereas more concentrated solutions (0.02–0.04 M) begin to favor the diligated species over the monoligated, as determined by careful analysis of the crystal morphologies and subsequent unit cell measurements. Interestingly, crystallizations of [AgL_2](OTf) did not produce noticeable amounts of [AgL](OTf); the equilibrium constant for eq 3 must be relatively large in all cases. It is conjectured that the lower solubility of [Ag(L)](OTf) versus [AgL_2](OTf) in THF (and the limiting L) allows isolation of the former by precipitation. Upon dissolution of pure [Ag(L)](OTf) in more polar solvents, equilibrium mixtures are obtained.

Second, NMR titrations of the ligands, L, with silver triflate (reverse of eq 2 and forward of eq 3) or of [AgL_2](OTf) with AgOTf (reverse of eq 4) in CD_3CN only gave one set of resonances (with different chemical shifts) regardless of the stoichiometry (see Figures S13 and S14 as examples) or the temperature within the solvent's liquid range, showing that these four species are in rapid equilibrium.

Third, the diffusion-oriented spectroscopy (DOSY) NMR experiments of various metal complexes of the new ligands were acquired at room temperature to provide further insight into their molecularity. Table 4 collects the diffusion constants, the hydrodynamic radii (calculated by using the Stokes–Einstein relation, as detailed in the Supporting Information), and the calculated radii from both X-ray diffraction studies and molecular modeling of the various ionic compounds. The data indicate that the complexes are most likely monomeric in CD_3CN at room temperature because the hydrodynamic radii of all silver(I) complexes are similar to one another (even those with dimeric and polymeric solid-state structures) and to those of the kinetically inert monomeric tricarbonylmanganese(I) complexes of the same ligands described later.

Table 4. Summary of the Data from ^{1}H NMR DOSY Experiments and Radii from the Longest Interatomic Distances in the Reference Structures or Models

compound	D ($\times 10^{-10}$ m^2/s)	r_{DOSY} (Å)	$r_{X\text{-}ray}$ (Å)	r_{model} (Å)	r_{model}(bonding)
$NBu_4(OTf)$	9.3(1)	5.7(2)	6.0[a]	5.9	
1a	7.0(9)	7.7(9)	6.5	6.8	κ^3 monomer
				7.5	κ^3, + CH_3CN
				8.7	κ^2, + CH_3CN
				11.3	κ^2,κ^1N dimer
1b	7.3(1)	7.2(1)	8.5	10.0	tetrahedral
2a	7.6(9)	7.8(8)		7.0	κ^3 monomer
				8.5	κ^2, + CH_3CN
				8.9	$Ag(^{Ts}L)_2$, tetrahedral
				11.3	κ^2,κ^1N dimer
			10.7	11.7	κ^1,κ^1N dimer
3a	9.0(9)	6.1(9)		6.0	κ^3 monomer
				6.3	κ^3, + CH_3CN
				7.4	$Ag(^{H}L^*)_2$, tetrahedral
			7.82	8.0	κ^2,κ^1N dimer
4a	7.9(4)	6.9(5)		5.33	κ^3 monomer
				7.45	κ^3, + CH_3CN
			7.10	6.7	$Ag(^{H}L)_2$, tetrahedral
				8.2	κ^2,κ^1N dimer
5	7.4(1)	7.1(2)		6.4	κ^3 monomer
8	8.3(1)	6.4(2)	5.8	6.1	κ^3 monomer

a Reference 61.

Next, the number and chemical shifts of the resonances in the NMR spectrum of each compound indicate that the complexes have dynamic solution structures that are different from their solid-state structures. Complexation of the ligands to cationic metal centers is characterized by a downfield shift in the “normal” pyrazolyl ring hydrogen H4 resonances, with respect to those in the free ligands. In every silver complex (and for the inert $[Mn(CO)_3]^+$ complexes described later), the “normal” pincer pyrazolyls have downfield-shifted H4 resonances and, hence, are silver-bound. For the “confused” pyrazolyl ring in each complex, the chemical shift of the resonance for the H5-ring hydrogen (next to the ring nitrogen’s tosyl or N–H group) indicates whether or not this heterocycle is metal-bound. In the spectra of each **3a**, **3b**, **4a**, and **4b** (with ^{H}L or ^{H}L*), the H5 resonance is shifted downfield, indicating that the “confused” ring is bound, whereas in the remaining cases (with ^{Ts}L or ^{Ts}L*), the chemical shift of this resonance matches that for the free ligand, so the confused ring is likely not bound. Thus, the ligands in **1a**, **3b**, and **4b** have different denticities in solution versus the solid state. It is reasonable that complexes **3b** and **4b** may be six-coordinate in solution given the sandwich structures of $[Ag(\kappa^3\text{-Tpm}^x)_2]^{2+}$ and the low energy barrier calculated for κ^2/κ^3-$[Ag(Tpm)]^+$ interconversions.[(49)] Considering the DOSY experiments, $[Ag(CH_3CN)_n(\kappa^{2\text{-}Ts}L^x)]^+$ (*n* = 1–2) would be possible for **1a** and **2a** (and by analogy for **3a**). These formulations do not include a silver-bound triflate because the spectroscopic data for each complex indicates a free (unbound) triflate anion in solution. That is, the ^{19}F NMR spectrum of each in CD_3CN shows only one resonance at −79.3 ppm that matches that for NBu_4OTf. It is also noteworthy that the solution IR spectra of each has one set of strong bands in the 1280–1025 cm^{-1} range for symmetric and asymmetric SO_3 and CF_3 stretching modes that are characteristic of an unbound triflate anion.[(50)] Thus, the solution structures of **1a**–**4a** with unbound triflates are different from the solid structures that showed silver-bound triflates. Although the triflate ion is not bound to silver in an acetonitrile solution, there is evidence for ion pairing in most cases, except **4a** and **4b**, from anomalous upfield shifts in certain hydrogen resonances, as seen with other metal complexes.[(51)] That is, for complexes **1a**, **1b**, **3a**, and **3b** with pz* groups, the resonance for the acidic methine, that for H_4 of the “confused” pyrazolyl ring, and that for one set of methyl pz* hydrogen atoms (closest to the methine) are unexpectedly shifted *upfield* from those in the spectrum of the free ligand. Given the different groups on the confused pyrazolyls and the propensity for triflate to be located near the methine positions of silver poly(pyrazolyl)methane complexes in the solid state,[(47)] it is likely that these hydrogen atoms are shielded by proximity to a nearby triflate ion. It is noted that the ^{1}H NMR spectrum of a concentrated mixture of NBu_4OTf and each charge-neutral ligand is a simple sum of the individual spectra of the pure components. Because the presence of the triflate does not affect the chemical shift of the charge-neutral ligands, ion pairing is essential for observation of the unusual upfield shifts (charge-assisted weak hydrogen bonding). In **2a** and **2b**, only the resonance for H_4 of the confused ring is significantly shifted upfield. It is unclear why upfield shifts were not observed in the spectrum of either **4a** or **4b**, which were of concentration similar to those of the other complexes. The simplicity of the ^{1}H NMR spectrum of **2a** also indicates that the static solid-state structure is not retained in solution. If it was retained, then two sets of resonances would be expected because the tosyl pyrazolyl arm points toward one of the “normal” pyrazolyls (see the right side of Figure 3) and would differentiate these heterocycles.

Fast free rotation about the $C_{methine}$–C bond of the “confused” pyrazolyl could explain equivalence at room temperature. Again, it was not possible to slow the dynamic behavior in the liquid range of CH_3CN. Given the results of the NMR titrations and the DOSY experiment described above, it is most likely that rather than retaining a dimeric solid-state structure, complex **2a** likely dissociates to a monomeric structure (eq 1), which then participates multiple fast dynamic equilibria according to eqs 2–4. Similarly, the spectrum of **4a** is simpler than expected based on the polymeric solid-state structure. There was only one set of sharp resonances for the “normal” pyrazolyls when two sets would be expected if the solid-state structure of **4a** remained intact and static in solution (those pyrazolyls in Figure 6 with N11 would be different from those with N21 by proximity to the confused pyrazolyl or to the pseudo-C_2 axis that passes through Ag3). In this case, direct dissociation (by breaking the Ag–N bonds on two-coordinate Ag) to give **4b** and AgOTf directly (eq 4) or dissociation to monomeric $[Ag(CH_3CN)_n(\kappa^3\text{-}^{H}L)]^+$ are reasonable possibilities.

Finally, ESI(+) MS spectral data of discrete complexes and coordination polymers of *inert* metal ions are generally accepted to be representative of solution structures.(52) Electrospray ionization is soft enough that labile complexes, including supramolecular species held together by noncovalent interactions, can also be measured by this technique.(53) The results described here, the extensive studies by the Reger group on the structures, and ESI(+) MS spectra of silver(I) poly(pyrazolyl)methane complexes demonstrate the existence of multiple solution species.(22, 54, 55) For instance, the ESI(+) MS spectrum of a solution of analytically pure **1a**, which had a monomeric $Ag(^{Ts}L^*)(OTf)$ solid structure, consists of a parent 100% relative abundance peak at *m*/*z* 329 for a ligand fragment ($^{Ts}L^*$ – pz*), a lower intensity peak (with 87% relative abundance) at *m*/*z* 957 for $[Ag(^{Ts}L^*)_2]^+$, and a still lower intensity peak (41% relative abundance) at *m*/*z* 531 for the expected parent ion, $[Ag(^{Ts}L^*)]^+$. Clearly, the $[Ag(^{Ts}L^*)_2]^+$ species could arise from a redistribution reaction (eq 4) or from the self-assembly of fragments that are already present in solution (eq 3) or, less likely, that are generated during ionizing conditions. Unfortunately, the peaks for $[Ag(CH_3CN)_n]^+$ (n = 3, 4) species were not observed in the *m*/*z* >200 spectral window. The mass spectrum of **1b** differs from that of **1a** only by the intensities of the peaks. Given the NMR titration data and the fact that mixtures of crystals are obtained from the crystallization of analytically pure **1a** in CH_3CN [the solvent also used in ESI(+) MS experiments], the ESI(+) MS data are indeed more likely representative of solution structures partitioned via eqs 2–4 rather than being representative of species generated during or after ionization. The mass spectral data for the remaining silver complexes agree with many (but not all) trends outlined previously by the Reger group on related systems. Thus, the spectra of **2a** and **3a**, which exhibit dimeric solid-state structures, feature weak-intensity (<30% relative abundance) peaks corresponding to $[Ag_2L_2(OTf)]^+$ and, for **3a**, to $[Ag_2(^{H}L^*)_2OTf$ – pz*$]^+$ and $[Ag_2(^{H}L^*)]^+$ (L* = deprotonated ligand). The highest-intensity peaks in each spectrum were for $[AgL_2]^+$ (100% relative abundance) and $[AgL]^+$ (>70% relative abundance). The lack of half-integer *m*/*z* peaks establishes the monomeric nature of the $[AgL]^+$ species. The mass spectrum of **4a**, which has a polymeric solid-state structure, displayed very weak intensity (<5% relative abundance) peaks for $[Ag_3(^{H}L)_3(OTf)_2]^+$, $[Ag_3(^{H}L)_2(OTf)_2]^+$, $[Ag_3(^{H}L)_2(OTf)(Cl)]^+$, $[Ag_3(^{H}L)(L)(OTf)]^+$, and $[Ag_3(L)_2]^+$, where L is a deprotonated ligand and Cl^- comes from the trace ions normally present in the mass spectrometer. There is also a series of higher-intensity

(between 5 and 40% relative abundance) peaks for dimeric monocationic species such as $[Ag_2(^{H}L)_2(OTf)]^+$ as well as disilver fragments $[Ag_2L(X)]^+$ (X = Cl, OTf). These peaks are rather unexpected because Reger had indicated that, in the cases of silver(I) poly(pyrazolyl)methanes with polymeric solid-state structures, peaks for dimeric units were notably absent.[54a, 54c] It may be possible that crystallization under different conditions may lead to a yet-to-be-discovered dimeric form of **4a**. As with the other three $[AgL]^+$ complexes, the most abundant peaks in the mass spectrum of **4a** were for $[Ag(^{H}L)_2]^+$ (95% relative abundance) and $[Ag(^{H}L)]^+$ (100% relative abundance). The origin of the relatively high abundance of monomeric monocations and decreasing abundance of higher-order monocations is most likely the result of the overall equilibrium constant of eqs 1–4. It is also noteworthy that the mass spectrum of **2b**, **3b**, or **4b** is devoid of peaks for disilver or other higher-order fragments. So, the equilibrium constant for eq 3 must again be relatively large.

Reactivity

The synthetic utility of the silver complexes as ligand delivery agents was demonstrated first via the preparation of tricarbonylmanganese(I) complexes (Scheme 4). The reactions between any of **1a**, **2a**, **3a**, or **4a** and $Mn(CO)_5Br$ in refluxing CH_3CN for 3 h gave high yields of **5**, **6**, **7**, or **8** as appropriate. Given the high yields and availability of silver complexes, no attempt was made to further improve the syntheses of **5**–**8** by performing the reaction in one pot (i.e., starting from free ligand, $Mn(CO)_5Br$, and AgOTf), although this may be a useful route. Complexes **5**–**8** are slightly light-sensitive yellow solids that are soluble in many organic solvents except hydrocarbons and Et_2O. Solutions of the complexes are noticeably more light-sensitive than the solids. So, solution characterization data were obtained only for freshly prepared solutions and with precautions to exclude light vide infra. The IR spectra of **5**–**8** (Table 5) give characteristic bands for the *fac*-$Mn(CO)_3$ moiety. That is, one sharp, higher-energy band and one broad, lower-energy band are found in the spectra of the solids. In CH_2Cl_2 solutions, the broad band is split to give three resolved bands in the cases of **5**–**7**; the local symmetry about manganese in **8** is probably high enough (C_{3v}) that the nominal *E* stretching mode is not split. The larger band broadening in the solids compared to solution likely does not allow resolution of any splitting in the broader band in this state. Also, as usual, the (weighted) average energies of the CO stretching frequencies in the solid are 10–20 cm^{-1} lower than those in solution. In either medium, complexes **5** and **7**, with 3,5-dimethylpyrazolyl donors, exhibit lower average CO stretching frequencies than **6** and **8** with unsubstituted pyrazolyls because the ligands in the former are stronger donors than those in the latter and increase the back-bonding capabilities of the manganese(I) center to the carbonyl. These findings are in agreement with those previously reported for $[(HC(pz^{R3,R5})_3)Mn(CO)_3](O_3SCF_3)$ (R = H, Me) (in CH_2Cl_2).[25] In the current complexes, the replacement of a tosyl group with a hydrogen has a marginal impact on the average CO stretching frequencies in a CH_2Cl_2 solution.

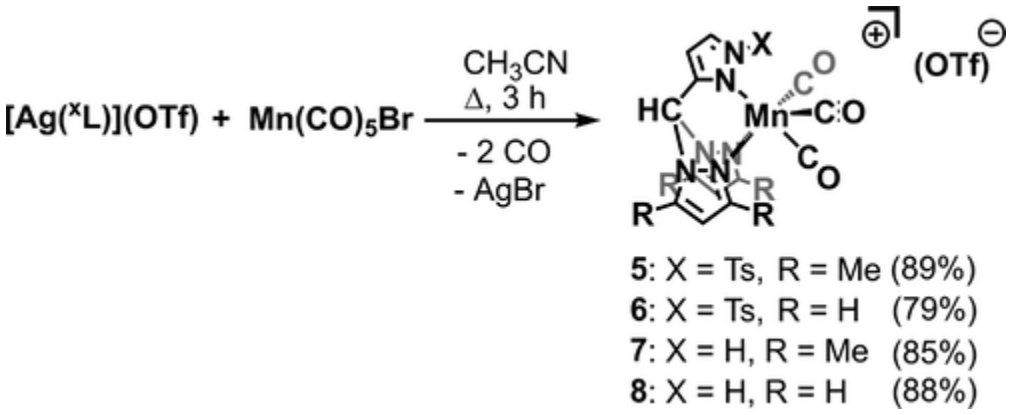

Scheme 4. Preparation of Tricarbonylmanganese(I) Complexes

Table 5. IR Spectral Data (CH_2Cl_2, KBr) for [(^{x}L)Mn(CO)$_3$](O_3SCF_3) Complexes

complex	ν_{CO} (cm^{-1})	ref
{[HC(pz*)$_3$]Mn(CO)$_3$}(OTf)	2044, 1949; wt avg = 1981	25
{[HC(pz)$_3$]Mn(CO)$_3$}(OTf)	2051, 1956; wt avg = 1988	25
5	2046, 1957, 1942; avg = 1982	this work
6	2052, 1965, 1952; avg = 1990	this work
7	2046, 1955, 1943; avg = 1981	this work
8	2050, 1955; wt avg = 1987	this work

The *fac* coordination mode was verified by X-ray diffraction for **6** and **8** (Figure 8 and Table 6). In each, the ligands exhibit κ^3N coordination to the metal center. In **6**, there are two independent cations in the asymmetric unit. In each, the Mn–N bond involving the tosyl pyrazolyl (avg 2.140 Å) is significantly longer than the other two Mn–N bonds (averaging 2.057 Å). The overall average Mn–N distance of 2.085 Å is longer than 2.07 Å found in [HC(3-iPrpz)$_3$)Mn(CO)$_3$](O_3SCF_3)(25) and 2.040 Å in [(PhCpz$_2$py)Mn(CO)$_3$](O_3SCF_3).(56) The disparity in the Mn–N distances also leads to a dichotomy in the Mn–C distances, where the Mn–C bond trans to the tosyl pyrazolyl (avg 1.805 Å) is shorter than the other two Mn–C bonds (avg 1.821 Å). There is no significant discrepancy in the C–O bond distances, which average at 1.141(3) Å. In **8**, the average Mn–N bond distance of 2.052 Å is shorter than that found for **6**, and the distances are more uniform, as might be expected after considering the relative steric demands of the “confused” pyrazolyls in each complex. The triflate anions in **6** and **8** are affixed to the cations via short CH···O (cyan dotted lines; Figure 8) and CH···F (green dotted lines; Figure 8) interactions and, in the case of **8**, NH···O weak hydrogen bonding (not shown) and serve to organize the three-dimensional supramolecular structure, as is more fully described in the Supporting Information.

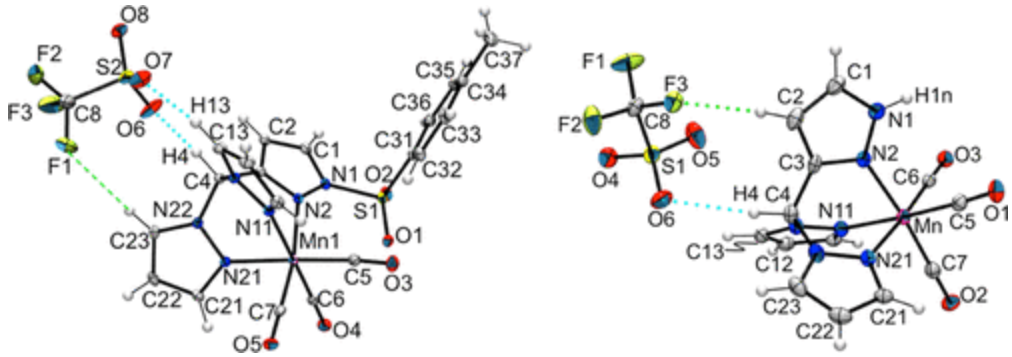

Figure 8. (Left) Structure of one of two symmetry independent units in the crystal of **6**. (Right) Structure of **8** with partial atom labeling.

Table 6. Selected Bond Distances (Å) and Angles (deg) in **6** and **8**

	6				**8**	
			Bond Distances (Å)			
Mn1–N2	2.1354(18)	Mn1a–N2a	2.149(2)		Mn1–N2	2.041(2)
Mn1–N11	2.0501(18)	Mn1a–N11a	2.0494(19)		Mn1–N11	2.058(2)
Mn1–N21	2.0652(18)	Mn1a–N21a	2.0613(19)		Mn1–N21	2.059(2)
Mn1–C5	1.822(2)	Mn1a–C5a	1.805(3)		Mn1–C5	1.807(3)
Mn1–C6	1.824(2)	Mn1a–C6a	1.826(2)		Mn1–C6	1.815(3)
Mn1–C7	1.803(2)	Mn1a–C7a	1.812(2)		Mn1–C7	1.812(3)
			Bond Angles (deg)			
N2–Mn1–N11	82.18(7)	N2a–Mn1a–N11a	81.89(7)		N2–Mn1–N11	84.08(10)
N2–Mn1–N21	83.47(7)	N2a–Mn1a–N21a	83.78(7)		N2–Mn1–N21	82.55(10)
N11–Mn1–N21	86.84(7)	N11a–Mn1a–N21a	86.07(7)		N11–Mn1–N21	84.86(9)
C5–Mn1–C6	89.98(10)	C5a–Mn1a–C6a	89.64(12)		C5–Mn1–C6	87.91(12)
C5–Mn1–C7	87.31(10)	C5a–Mn1a–C7a	85.08(11)		C5–Mn1–C7	91.49(13)
C6–Mn1–C7	90.17(10)	C6a–Mn1a–C7a	90.01(11)		C6–Mn1–C7	89.54(12)
C5–Mn1–N2	99.57(8)	C5a–Mn1a–N2a	172.24(10)		C5–Mn1–N2	92.52(11)
C5–Mn1–N11	91.86(8)	C5a–Mn1a–N11a	92.45(10)		C5–Mn1–N11	176.59(11)
C5–Mn1–N21	176.51(9)	C5a–Mn1a–N21a	90.55(10)		C5–Mn1–N21	94.71(11)
C6–Mn1–N2	95.95(8)	C6a–Mn1a–N2a	95.80(9)		C6–Mn1–N2	94.33(11)
C6–Mn1–N11	177.57(9)	C6a–Mn1a–N11a	176.88(9)		C6–Mn1–N11	92.35(11)
C6–Mn1–N21	91.42(9)	C6a–Mn1a–N21a	91.59(9)		C6–Mn1–N21	176.01(10)
C7–Mn1–N2	170.76(8)	C7a–Mn1a–N2a	100.41(9)		C7–Mn1–N2	174.52(11)
C7–Mn1–N11	90.17(10)	C7a–Mn1a–N11a	92.48(9)		C7–Mn1–N11	91.91(12)
C7–Mn1–N21	89.48(9)	C7a–Mn1a–N21a	175.34(10)		C7–Mn1–N21	93.40(11)

In a CD_3CN solution, the NMR spectra for each **7** and **8** were in accordance with expectations of complexes with κ^3N ligands coordinated to the *fac*-$Mn(CO)_3$ fragment. At room temperature, the resonances for ligand hydrogen atoms are broadened slightly by the quadrupolar ^{55} Mn

nucleus (I = $^5/_2$, 100%) but sharpen upon heating. All resonances are shifted downfield from those found in the free ligand. The spectrum of each **5** and **6** in CD_2Cl_2 or acetone-d_6 is in accordance with expectations, but those in CD_3CN are more complicated than expected because two sets of resonances in a 5:1 ratio are observed. The major resonances agree with the expectations for a κ^3N-ligated species, where all resonances for ligand hydrogen nuclei are shifted downfield compared to those of the free ligand. The minor resonances all have downfield-shifted resonances except for those of the confused pyrazolyl, which are shifted upfield from those in the free ligand. It is likely that the minor species has a dissociated tosylpyrazolyl group and a solvent bound to the metal instead. Because of the different relaxation times of the ^{13}C nuclei versus ^{1}H, the ^{13}C NMR spectra of **7** and **8** are not broadened. The resonances for the carbonyl carbon atoms are observed at room temperature near 221 and 215 ppm, consistent with the chemical shifts reported for the tricarbonylmanganese(I) complexes of tris(pyrazolyl)methane derivatives.[(25)] The electronic absorption spectrum of each of **5**–**8** consists of a medium-intensity ($\varepsilon \sim 2500$ M^{-1} cm^{-1}), low-energy metal-to-ligand charge-transfer (MLCT) band (d_{Mn}–π^*_{CO}) with λ_{max} near 360 nm that trails into the violet, which is responsible for the yellow color of the complexes. The intraligand transitions are found at higher energy. The light sensitivity of the complexes is likely due to the known photoactivated CO-releasing properties of $[(HCpz_3)Mn(CO)_3]^+$ and related complexes (thereby removing the chromophore).[(57)] This property is outside the scope of the current work, so it was not investigated further here.

The use of silver complexes as stoichiometric ligand delivery agents was also demonstrated in the preparation of the iron(II) complex **9** by two routes (Scheme 5). First, the metathesis reaction between a MeOH solution of **4a** (2 equiv) and an aqueous solution of $FeCl_2$ (1 equiv) gave a high yield of pure **9** after the simple removal of AgCl by filtration and solvent under vacuum. Alternatively, a lower yield of **9** was obtained by the redox reaction between 2 equiv of **4a** and the iron metal in CH_3CN. The lower yield of this latter route was a result of both incomplete reaction and difficulties associated with separating **9** from residual **4a** by fractional crystallization. It is noted that the direct reaction between 2 equiv of ligand and commercial $Fe(OTf)_2$ to give **9** gave a lower yield than the metathetical route because of issues with the solubility of the reagents, as well as the difficulties in separating the product from an unidentified yellow intermediate. Thus, the alternative routes to **9** proved useful when unexpected difficulties occurred in the direct reaction and could be useful in the future with certain cases where a metal triflate salt is not readily available or is more expensive than a metal halide or elemental metal (cobalt, for instance).

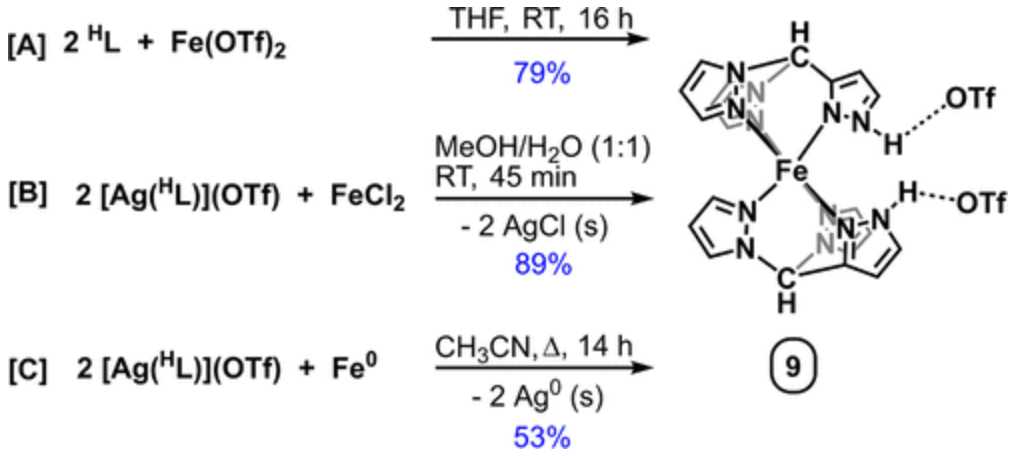

Scheme 5. Preparative Routes to **9**

Vapor diffusion of Et_2O into a MeOH solution of **9** gave crystals suitable for X-ray diffraction. The structure of **9** obtained at 100 K is given in Figure 9. The complex crystallizes as a cis isomer in the *P*2/*c* space group, where iron resides on a C_2 crystallographic axis that bisects the "confused" pyrazolyls through the iron, giving only three inequivalent Fe–N bonds in the FeN_6 kernel. The Fe1–N2 bond of the "confused" pyrazolyl of 1.941(3) Å is shorter than the similar bonds of the other two pyrazolyls (Fe1–N11 = 1.978(3) Å and Fe1–N21 = 1.983(3) Å), and all are consistent with low-spin rather than high-spin iron(II). The triflate counterions are affixed to the dication via charge-assisted weak hydrogen bonding with the confused pyrazolyl (N1–H1n···O3, 2.025 Å, 176°). Further weak CH···O interactions between the triflate oxygen and acidic (methine and pyrazolyl) hydrogen atoms of neighboring dications serve to organize the three-dimensional supramolecular structure, as detailed in Figure S12.

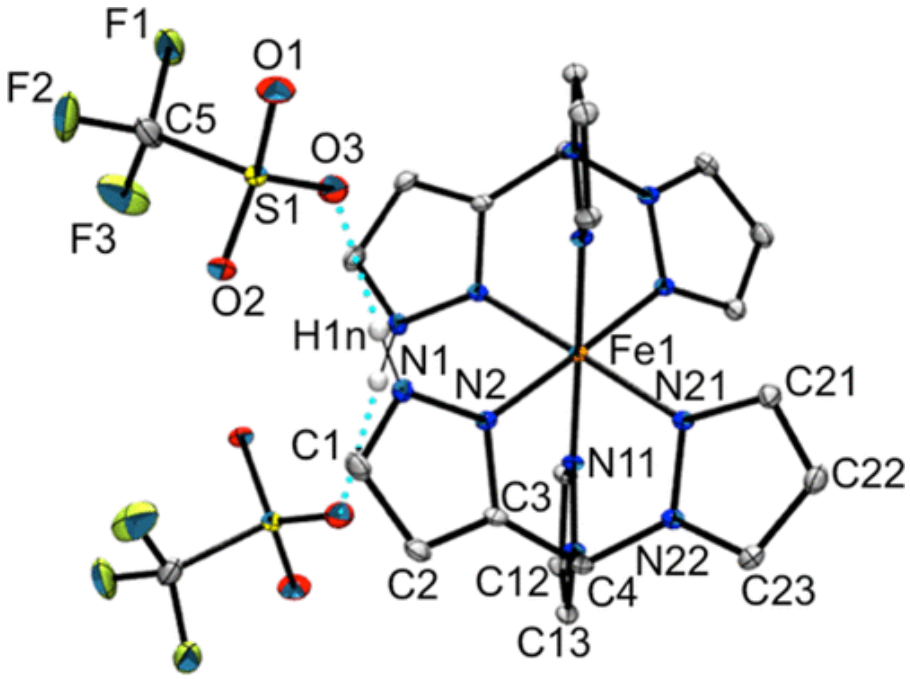

Figure 9. Structure of **9** with most hydrogen atoms removed for clarity.

Although complex **9** is pink, a color characteristic of low-spin iron(II), it is slightly paramagnetic at room temperature. Crystalline or powder samples reversibly change between pink and colorless upon cycling between heating to 150 °C and then cooling to room temperature. This behavior is similar to that of $[Fe(^{H}L)_2](BF_4)_2$ (**10**), a compound that showed a gradual (from S = 0 to 2) spin transition with $T_{1/2}$ near 360 K (beginning at ca. 275 K and is only 80% complete at 400 K).[(31)] The solid-state magnetic behavior of **9** (Figure 10) shows a spin transition $T_{1/2}$ near 365 K, but the spin-crossover (SCO) is more abrupt than that in **10**. The SCO in **9** begins at ca. 330 K and reaches ca. 95% completion at 400 K. Weak charge-assisted hydrogen bonding organizes the solid-state structure in each **9** and **10**. Clearly, the abruptness of the $\chi_M T$ versus T curve in the 300–400 K range indicates that the NH···O and CH···O interactions in **9** are stronger that the NH···F and CH···F interactions in **10**, as might be expected. It is also noteworthy that solutions of **9** are also slightly paramagnetic despite being pink. The solution magnetic moment of 2.0 μ_B (Evan's method) for **9** in CD_3OD at 295 K is indicative of a significant fraction of high-spin iron(II) and is similar to the solid-state magnetic moment at 295 K. The electronic absorption spectrum shows characteristic bands for d–d transitions, MLCT bands of low-spin iron, and a very weak feature in the near-IR (ca. 9000 cm^{-1}) for the weak d–d transition for high-spin iron(II).

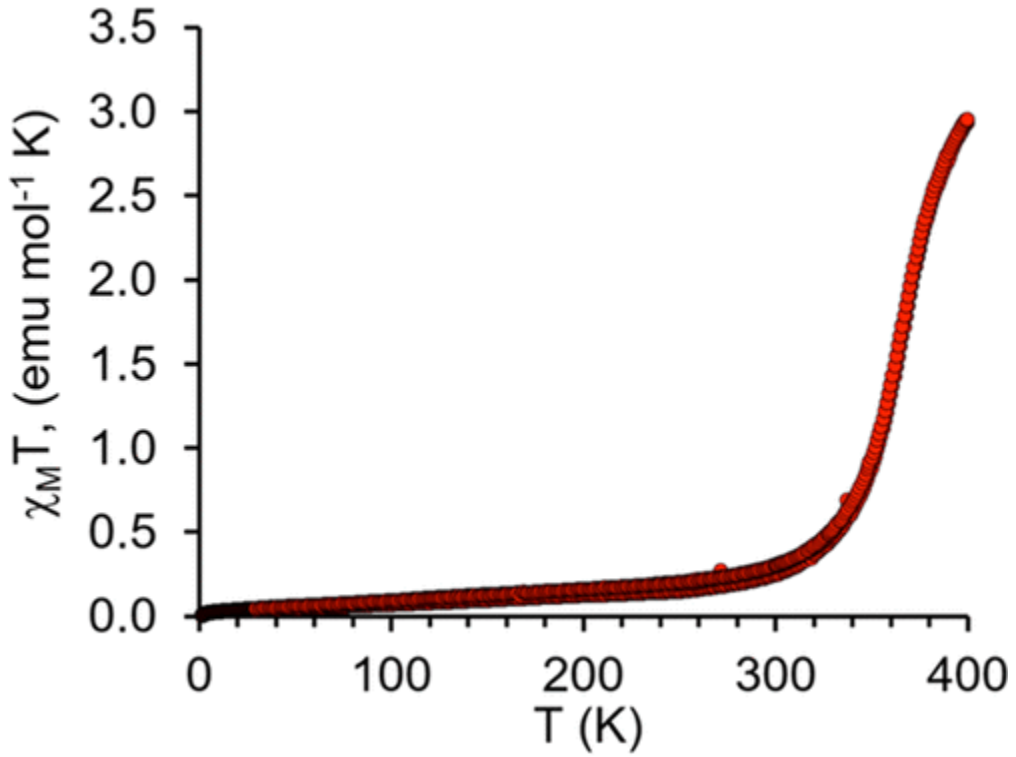

Figure 10. Temperature dependence of $\chi_M T$ for **9** from SQUID magnetometry.

Nitrene-Transfer Catalysis

The ability for the new silver complexes to catalyze nitrene transfer at 2 mol % loading was probed by the reaction between styrene, *N*-tosylamine, and a commercial hypervalent iodine reagent, $PhI(OAc)_2$, in CH_3CN. Table 7 summarizes the results of these initial investigations.

Surprisingly, the best-performing catalyst of those tested was **1b** followed by **1a ≈ 2a** and then **3a**. The other new silver complexes performed similarly to control experiments that show activated molecular sieves alone have some activity under these conditions (16 h at 80 °C). It is noted that the aziridination reactions did not proceed either at room temperature, in CH_2Cl_2, or even when using preformed PhI═NTs (as in other silver-catalyzed aziridination reactions). For those complexes that successfully catalyzed the aziridination of styrene, the use of strictly anhydrous silver triflate (for in situ reactions) or oven-dried samples of preformed complexes was crucial for ensuring both reproducibility and maximum activity (as reported in other cases). Interestingly, in the reactions where catalysis was successful, a small amount (1–2%) of a statistical diastereomeric mixture of 2,4-diphenyl-*N*-tosylpyrrolidine (B; see Table 7) was also identified [by ^{1}H NMR and ESI(+) MS; see Figures S17 and S18]. This side product, B, is a result of [3 + 2] cycloaddition between styrene and 2-phenyl-*N*-tosylaziridine (A). While this particular transformation has been reported to be catalyzed by manganese(III) tetraphenylporphyrin,(36) to our knowledge, it has never previously been effected by a silver(I) complex. However, [3 + 2] cycloadditions between aziridines and either alkynes,(58) aldehydes,(59) or naphthols(60) are known to be catalyzed (or promoted) by $AgSbF_6$ or AgOTf. Control reactions on the NMR scale showed that heating a mixture of styrene and aziridine did not lead to any productive transformation (other than the slow formation of polystyrene). The addition of **1a** also did not give pyrrolidine (B). Clearly, the presence of the byproduct requires the oxidant and heating at 80 °C. The higher activity of **1b** versus **1a** in aziridination is rather surprising, considering the relative reactivity of the remaining complexes that favor complexes with 1:1 rather than 2:1 ligand/metal ratios. It can be speculated that both $[AgL]^+$ and $[AgL_2]^+$ may catalyze the reactions (and both exist in solution via eqs 1–4), but the larger steric requirements of ^{Ts}L* decrease the likelihood for the diligated species to adopt a six-coordinate (and presumably catalytically inactive) silver center in solution. Future experimental and computational efforts will be directed toward determining the mechanism of catalysis and whether altering ligand sterics or electronics can give silver *C*-scorpionate catalysts that are more competitive with the $AgTp^x$ or other silver catalysts for aziridination reactions.

Table 7. Summary of Results from Nitrene-Transfer Reactions[a]

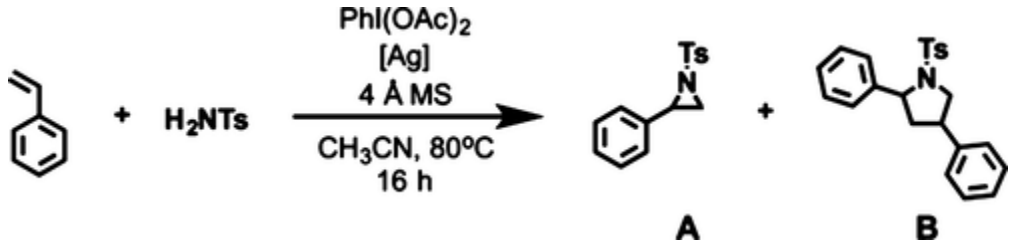

entry	[Ag]	NMR yield of A	% yield of A[b]	% yield of B[b]	TON[c]
1	none	3 (2)	0	0	0
2	AgOTf	3 (2)	0	0	0
3	**1a**	17 (6)	18 (5)	2.2 (0.1)	10
4	**1b**	34 (4)	27 (3)	2 (1)	15
5	**1b**[d]	27 (3)			

entry	[Ag]	NMR yield of A	% yield of A[b]	% yield of B[b]	TON[c]
6	**2a**	16 (8)	10 (2)	2.1 (0.5)	11
7	**2a**[e]	trace			
8	**2b**	6 (2)	8 (2)	0	4
9	**3a**	15 (3)	12 (4)	1 (0.2)	7
10	**3b**	6 (1)			
11	**4a**	8 (2)	2	0	1
12	**4b**[d]	6 (1)			

A Conditions: 5 mmol of styrene, 1 mmol of $PhI(OAc)_2$, 1 mmol of H_2NTs, 0.02 mmol fo [Ag], 0.5 g of 4 Å molecular sieves, 4 mL of CH_3CN, 16 h, 80 °C.
B Isolated yields based on H_2NTs; average of three runs (average deviation in parentheses).
C TON = mmol (A + B, isolated)/mmol [Ag].
D In situ.
E Room temperature, 16 h.

Conclusions

Two new N-confused *C*-scorpionate ligands with 3,5-dimethylpyrazolyl “pincers” and either an *N*-tosyl (^{Ts}L*) or an N–H (^{H}L*) “stinger” have been prepared in high yield. Together with the previously known, less bulky derivatives, a complete set of four nitrogen-confused scorpionate ligands with a wide range of steric profiles is now available for coordination chemistry studies. It was possible to structurally characterize the complete set of eight silver complexes that had both 1:1 and 2:1 L/Ag ratios. In the solid state, the 2:1 complexes had four-coordinate silver by binding only the pincers; the confused scorpionate stinger was not bound. This is a remarkable finding in light of the structures of the $[Ag(Tpm^x)_2]^+$ complexes that showed only six-coordinate sandwich structures and of theoretical studies that showed a barrierless transition from κ^2-Tpm to κ^3-Tpm complexation. Steric bulk and electronic effects may both favor the formation of four-coordinate complexes of the N-tosylated ligands, while stabilization through hydrogen-bonding interactions in the solid state may play an integral role for $[Ag(^{H}L^*)_2]^+$ and $[Ag(^{H}L)_2]^+$. In 1:1 complexes, the bulkiest derivative, ^{Ts}L*, gave a monomeric species, the least bulky derivative, ^{H}L, gave a polymeric species and the other two ligands of medium steric profiles gave dimeric complexes in the solid state. The ^{1}H NMR, DOSY NMR, and ESI(+) MS spectral studies indicate that the solid-state structures are not preserved in solution. Rather, all have dynamic solution behavior and are involved in multiple rapid equilibria. The labile nature of silver(I) complexes is expected and allows for the use of silver(I) complexes as effective ligand delivery agents. This property was demonstrated by the preparation of tricarbonylmanganese(I) complexes and **9**, a complex with SCO properties. Also, for the first time, the use of silver(I) *C*-scorpionates as nitrene-transfer catalysts has been demonstrated by the aziridination of styrene in CH_3CN using H_2NTs and $PhI(OAc)_2$ as oxidants. The activity of these species is low especially compared to those reported for $AgTp^x$ complexes probably because of the more complex solution behavior of the former, including the possibility for coordination to ions.

Acknowledgment

J.R.G. thanks Marquette University for support.

References

1 (a) Trofimenko, S. Scorpionates: The Coordination Chemistry of Polypyrazolylborate Ligands; Imperial Press: London, 1999. (b) Pettinari, C. Scorpionates II: Chelating Borate Ligands; Imperial Press: London, 2008.

2 Spicer, M. D.; Reglinski, J. Soft Scorpionate Ligands Based on Imidazole-2-thione Donors Eur. J. Inorg. Chem. 2009, 12, 1553– 1574 DOI: 10.1002/ejic.200801240

3 (a) Alkorta, I.; Claramunt, R. M.; Díez-Barra, E.; Elguero, J.; de la Hoz, A.; Lopez, C. The Organic Chemistry of Poly(1*H*-pyrazol-1-yl)methanes Coord. Chem. Rev. 2017, 339, 153– 182 DOI: 10.1016/j.ccr.2017.03.011 (b) Pettinari, C.; Pettinari, R. Metal Derivatives of Poly(pyrazolyl)alkanes: 1. Tris(pyrazolyl)alkanes and related systems Coord. Chem. Rev. 2005, 249, 525– 543 DOI: 10.1016/S0010-8545(04)00131-6 (c) Bigmore, H. R.; Lawrence, S. C.; Mountford, P.; Tredget, C. S. Coordination, organometallic and related chemistry of tris(pyrazolyl)methane ligands Dalton Trans. 2005, 635– 651 DOI: 10.1039/b413121e (d) Reger, D. L. Tris(pyrazolyl)methane ligands: the neutral analogs of tris(pyrazolyl)borate ligands Comments Inorg. Chem. 1999, 21, 1– 28 DOI: 10.1080/02603599908020413

4 (a) Kläui, W.; Berghahn, M.; Rheinwald, G.; Lang, H. Tris(pyrazolyl)methanesulfonates: A Novel Class of Water-Soluble Ligands Angew. Chem., Int. Ed. 2000, 39, 2464– 2466 DOI: 10.1002/1521-3773(20000717)39:14<2464::AID-ANIE2464>3.0.CO;2-5 (b) Kläui, W.; Schramm, D.; Peters, W.; Rheinwald, G.; Lang, H. Tris(pyrazolyl)methanesulfonate (Tpms) – A Versatile Alternative to Tris(pyrazolyl)borate in Rhodium(I) Chemistry Eur. J. Inorg. Chem. 2001, 2001, 1415– 1424 DOI: 10.1002/1099-0682(200106)2001:6<1415::AID-EJIC1415>3.0.CO;2-Z (c) Kläui, W.; Berghahn, M.; Frank, W.; Reiβ, G. J.; Schönherr, T.; Rheinwald, G.; Lang, H. Tris(pyrazolyl)methanesulfonates: More Than Just Analogues of Tris(pyrazolyl)borate Ligands; N,N,N-, N,N,O-, and Other Coordination Modes Eur. J. Inorg. Chem. 2003, 2003, 2059– 2070 DOI: 10.1002/ejic.200200604 (d) Papish, E. T.; Taylor, M. T.; Jernigan, F. E., 3rd; Rodig, M. J.; Shawhan, R. R.; Yap, G. P. A.; Jove, F. A. Synthesis of zinc, copper, nickel, cobalt, and iron complexes using tris(pyrazolyl)methane sulfonate ligands: a structural model for N,N,O binding in metalloenzymes Inorg. Chem. 2006, 45, 2242– 2250 DOI: 10.1021/ic051579a

5 Pettinari, C.; Cingolani, A.; Lobbia, G. G.; Marchetti, F.; Martini, D.; Pellei, M.; Pettinari, R.; Santini, C. Copper and Silver Derivatives of Scorpionates and Related Ligands Polyhedron 2004, 23, 451– 469 DOI: 10.1016/j.poly.2003.11.033

6 Other reviews: (a) Caballero, Ana; Mar Díaz-Requejo, M.; Fructos, M. R.; Urbano, Juan; Pérez, P. J. Modern Applications of Trispyrazolylborate Ligands in Coinage Metal Catalysis. In Ligand Design in Metal Chemistry: Reactivity and Catalysis; Stradiotto, M.; Lundgren, R. J., Eds.; John Wiley & Sons, Ltd.: Chichester, U.K., 2016; pp 308– 329; DOI: 10.1002/9781118839621.ch11 . (b) Pettinari, C.; Pettinari, R.; Marchetti, F. Golden Jubilee for Scorpionates: Recent Advances in Organometallic Chemistry and Their Role

in Catalysis Adv. Organomet. Chem. 2016, 65, 175– 260 DOI: 10.1016/bs.adomc.2016.01.002 (c) Caballero, A.; Perez, P. Catalyst design in the alkane C-H bond functionalization of alkanes by carbene insertion with Tp^xM complexes (Tpx = hydrotrispyrazolylborate ligand; M = Cu, Ag) J. Organomet. Chem. 2015, 793, 108– 113 DOI: 10.1016/j.jorganchem.2015.02.029 (d) Diaz-Requejo, M. M.; Perez, P. J. Coinage Metal Catalyzed C-H Bond Functionalization of Hydrocarbons Chem. Rev. 2008, 108, 3379– 3394 DOI: 10.1021/cr078364y (e) Diaz-Requejo, M. M.; Perez, P. J. Copper, silver and gold-based catalysts for carbene addition or insertion reactions J. Organomet. Chem. 2005, 690, 5441– 5450 DOI: 10.1016/j.jorganchem.2005.07.092

7 Dias, H. V. R.; Browning, R. G.; Polach, S. A.; Diyabalanage, H. V. K.; Lovely, C. J. Activation of Alkyl Halides via a Silver-Catalyzed Carbene Insertion Process J. Am. Chem. Soc. 2003, 125, 9270– 9271 DOI: 10.1021/ja034801o

8 Lovely, C. J.; Browning, R. G.; Badarinarayana, V.; Dias, H. V. R. A Silver-Catalyzed Büchner Reaction Tetrahedron Lett. 2005, 46, 2453– 2455 DOI: 10.1016/j.tetlet.2005.02.052

9 Dias, H. V. R.; Browning, R. G.; Richey, S. A.; Lovely, C. J. Silver(I) Scorpionate Mediated Insertion of Carbenes into Aliphatic C-H Bonds Organometallics 2004, 23, 1200– 1202 DOI: 10.1021/om0499198

10 (a) Alvarez, M.; Gava, R.; Rodriguez, M. R.; Rull, S. G.; Perez, P. J. Water as the Reaction Medium for Intermolecular C–H Alkane Functionalization in Micellar Catalysis ACS Catal. 2017, 7, 3707– 3711 DOI: 10.1021/acscatal.6b03669 (b) Caballero, A.; Despagnet-Ayoub, E.; Mar Diaz-Requejo, M.; Diaz-Rodriguez, A.; Gonzalez-Nunez, M. E.; Mello, R.; Munoz, B. K.; Ojo, W.-S.; Asensio, G.; Etienne, M.; Perez, P. J. Silver-Catalyzed C-C Bond Formation Between Methane and Ethyl Diazoacetate in Supercritical CO_2 Science 2011, 332, 835– 838 DOI: 10.1126/science.1204131 (c) Despagnet-Ayoub, E.; Jacob, K.; Vendier, L.; Etienne, M.; Alvarez, E.; Caballero, A.; Diaz-Requejo, M. M.; Perez, P. J. A New Perfluorinated F21-Tp Scorpionate Ligand: Enhanced Alkane Functionalization by Carbene Insertion with (F21-Tp)M Catalysts (M = Cu, Ag) Organometallics 2008, 27, 4779– 4787 DOI: 10.1021/om800531a (d) Gomez-Emeterio, B. P.; Urbano, J.; Diaz-Requejo, M. M.; Perez, P. J. Easy Alkane Catalytic Functionalization Organometallics 2008, 27, 4126– 4130 DOI: 10.1021/om800218d (e) Braga, A. A. C.; Maseras, F.; Urbano, J.; Caballero, A.; Diaz-Requejo, M. M.; Perez, P. J. Mechanism of Alkane C-H Bond Activation by Copper and Silver Homoscorpionate Complexes Organometallics 2006, 25, 5292– 5300 DOI: 10.1021/om060445h (f) Urbano, J.; Belderrain, T. R.; Nicasio, M. C.; Trofimenko, S.; Diaz-Requejo, M. M.; Perez, 11 P. J. Functionalization of Primary Carbon-Hydrogen Bonds of Alkanes by Carbene Insertion with a Silver-Based Catalyst Organometallics 2005, 24, 1528– 1532 DOI: 10.1021/om050024k

12 Iglesias, M. J.; Nicasio, M. C.; Caballero, A.; Perez, P. J. Silver-catalyzed silicon-hydrogen bond functionalization by carbene insertion Dalton Trans. 2013, 42, 1191– 1195 DOI: 10.1039/C2DT31460F

13 Urbano, J.; Braga, A. A. C.; Maseras, F.; Alvarez, E.; Diaz-Requejo, M. M.; Perez, P. J. The mechanism of the catalytic functionalization of haloalkanes by carbene insertion: an

experimental and theoretical study Organometallics 2009, 28, 5968– 5981 DOI: 10.1021/om9006888
14 Rivilla, I.; Sameera, W. M. C.; Alvarez, E.; Diaz-Requejo, M. M.; Maseras, F.; Perez, P. J. Catalytic cross-coupling of diazo compounds with coinage metal-based catalysts: an experimental and theoretical study Dalton Trans. 2013, 42, 4132– 4138 DOI: 10.1039/c2dt32439c
15 Maestre, L.; Sameera, W. M. C.; Díaz-Requejo, M. M.; Maseras, F.; Pérez, P. J. A general mechanism for the copper-and silver-catalyzed olefin aziridination reactions: Concomitant involvement of the singlet and triplet pathways J. Am. Chem. Soc. 2013, 135, 1338– 1348 DOI: 10.1021/ja307229e
16 Llaveria, J.; Beltran, A.; Diaz-Requejo, M. M.; Matheu, M. I.; Castillon, S.; Perez, P. J. Efficient Silver-Catalyzed Regio- and Stereospecific Aziridination of Dienes Angew. Chem., Int. Ed. 2010, 49, 7092– 7095 DOI: 10.1002/anie.201003167
17 Beltrán, A.; Lescot, C.; Díaz-Requejo, M. M.; Pérez, P. J.; Dauban, P. Catalytic C-H amination of alkanes with sulfonimidamides: Silver(I)-scorpionates vs. dirhodium(II) carboxylates Tetrahedron 2013, 69, 4488– 4492 DOI: 10.1016/j.tet.2013.02.005
18 Maestre, L.; Dorel, R.; Pablo, Ó.; Escofet, I.; Sameera, W. M. C.; Álvarez, E.; Maseras, F.; Díaz-Requejo, M. M.; Echavarren, A. M.; Pérez, P. J. Functional group tolerant, Silver-catalyzed N-N bond formation by Nitrene Transfer to amines J. Am. Chem. Soc. 2017, 139, 2216– 2223 DOI: 10.1021/jacs.6b08219
19 Lam, T. L.; Tso, K. C. – H; Cao, B.; Yang, C.; Chen, D.; Chang, X. – Y.; Huang, J. – S.; Che, C. – M. Tripodal S-Ligand Complexes of Copper(I) as Catalytsts for Alkene Aziridination, Sulfide Sulfimidation and C-H Amidination Inorg. Chem. 2017, 56, 4253– 4257 DOI: 10.1021/acs.inorgchem.7b00226
20 Arenas, I.; Fuentes, M. A.; Álvarez, E.; Díaz, Y.; Caballero, A.; Castillón, S.; Pérez, P. J. Syntheses of a Novel Fluorinated Trisphosphinoborate Ligand and Its Copper and Silver Complexes. Catalytic Activity toward Nitrene Transfer Reactions Inorg. Chem. 2014, 53, 3991– 3999 DOI: 10.1021/ic4028223
21 (a) Smolenski, P.; Pettinari, C.; Marchetti, F.; Guedes da Silva, M. F. C.; Lupidi, G.; Badillo Patzmay, G. V.; Petrelli, D.; Vitali, L. A.; Pombeiro, A. J. L. Syntheses, structures, and antimicrobial activity of new remarkably light-stable and water-soluble tris(pyrazolyl) methanesulfonate silver(I) derivatives of N-methyl-1, 3, 5-triaza-7-phosphaadamantane salt - [mPTA] BF_4 Inorg. Chem. 2015, 54, 434– 440 DOI: 10.1021/ic501855k (b) Pettinari, C.; Marchetti, F.; Lupidi, G.; Quassinti, L.; Bramucci, M.; Petrelli, D.; Vitali, L. A.; Guedes da Silva, M. F. C.; Martins, L. M. D. R. S.; Smolenski, P.; Pombeiro, A. J. L. Synthesis, Antimicrobial and Antiproliferative Activity of Novel 22 Silver(I) Tris(pyrazolyl)methanesulfonate and 1, 3, 5-Triaza-7-phosphadamantane Complexes Inorg. Chem. 2011, 50, 11173– 11183 DOI: 10.1021/ic201714c
23 Cingolani, A.; Effendy; Martini, D.; Pellei, M.; Pettinari, C.; Skelton, B. W.; White, A. H. Silver Derivatives of Tris(pyrazol-1-yl)methanes. A silver(I) nitrate complex containing tris(pyrazolyl)methane coordinated in a bridging mode Inorg. Chim. Acta 2002, 328, 87– 95 DOI: 10.1016/S0020-1693(01)00690-9

24 (a) Reger, D. L.; Collins, J. E.; Rheingold, A. L.; Liable-Sands, L. M.; Yap, G. P. A. Syntheses and Characterization of cationic (Tris(pyrazolyl)methane)Silver(I) Complexes. Solid State Structures of {[HC(3,5-$Me_2pz)_3]_2Ag$}(O_3SCF_3), {[HC(3$Bu^tpz)_3]_2Ag$}(O_3SCF_3), and {[HC(3$Bu^tpz)_3]_2Ag(CNBu^t$}(O_3SCF_3) Organometallics 1997, 16, 349– 353 DOI: 10.1021/om960481o (b) Reger, D. L.; Semeniuc, R. F.; Smith, M. D. Influence of the Crystallization Solvent on Molecular and Supramolecular Structures of Silver(I) Tris(3-Phenylpyrazolyl)methane Complexes Eur. J. Inorg. Chem. 2003, 2003, 3480– 3494 DOI: 10.1002/ejic.200300141 (c) Semeniuc, R. F.; Reger, D. L. Metal Complexes of Multitopic, Third Generation Poly(pyrazolyl)-methane Ligands: Multiple Coordination Arrangements Eur. J. Inorg. Chem. 2016, 2016, 2253– 2271 DOI: 10.1002/ejic.201600116

25 Hückel, W.; Chneider, H. B. N-Tripyrazolyl-methan Ber. Dtsch. Chem. Ges. B 1937, 70, 2024– 2026 DOI: 10.1002/cber.19370700931

26 Julia, S.; del Mazo, J.; Avila, L.; Elguero, J. Improved Synthesis Of Polyazolylmethanes Under Solid-Liquid Phase-Transfer Catalysis Org. Prep. Proced. Int. 1984, 16, 299– 307 DOI: 10.1080/00304948409457886

27 Reger, D. L.; Grattan, T. C.; Brown, K. J.; Little, C. A.; Lamba, J. J. S.; Rheingold, A. L.; Sommer, R. D. Syntheses of tris(pyrazolyl)methane ligands and {[tris(pyrazolyl)methane]$Mn(CO)_3$}SO_3CF_3 complexes: Comparison of Ligand Donor Properties J. Organomet. Chem. 2000, 607, 120– 128 DOI: 10.1016/S0022-328X(00)00290-4

28 Li, Z.; Capretto, D. A.; He, C. Silver- Mediated Oxidation Reactions: Recent Advances and New Prospects Prog. Inorg. Chem. 2009, 56, 1– 48 DOI: 10.1002/9780470440124.ch1 (b) Li, Z.; Capretto, D. A.; Rahaman, R.; He, C. Silver-Catalyzed Intermolecular Amination of C-H Groups Angew. Chem., Int. Ed. 2007, 46, 5184– 5186 DOI: 10.1002/anie.200700760 (c) Li, Z.; He, C. Recent Advances in Silver-Catalyzed Nitrene, Carbene, and Silylene-Transfer Reactions Eur. J. Org. Chem. 2006, 2006, 4313– 4322 DOI: 10.1002/ejoc.200500602 (d) Cui, Y.; He, C. A Silver-Catalyzed Intramolecular Amidation of Saturated C-H Bonds Angew. Chem., Int. Ed. 2004, 43, 4210– 4212 DOI: 10.1002/anie.200454243 (e) Cui, Y.; He, C. Efficient Aziridination of Olefins Catalyzed by a Unique Disilver(I) Compound J. Am. Chem. Soc. 2003, 125, 16202– 16203 DOI: 10.1021/ja038668b

29 (a) Yang, M.; Su, B.; Wang, Y.; Chen, K.; Jiang, X.; Zhang, Y. – F.; Zhang, X. – S.; Chen, G.; Cheng, Y.; Cao, Z.; Guo, Q. – Y.; Wang, L.; Shi, Z. – J. Silver-Catalyzed Direct Aminatino of Unactivated C-H Bonds of Functionalized Molecules Nat. Commun. 2014, 5, 4707 DOI: 10.1038/ncomms5707 (b) Zhang, X. Mechanistic Study on Silver-catalyzed Direct Amination of Unactivated C-H Bond J. Organomet. Chem. 2017, 832, 1– 8 DOI: 10.1016/j.jorganchem.2017.01.006

30 (a) Corbin, J. R.; Schomaker, J. M. Tunable differentiation of tertiary C-H bonds in intramolecular transition metal-catalyzed nitrene transfer reactions Chem. Commun. 2017, 53, 4346– 4349 DOI: 10.1039/C7CC01235G (b) Alderson, J. M.; Corbin, J. R.; Schomaker, J. M. Tunable, Chemo- and Site Selective Nitrene Transfer Reactions through the Rational Design of Silver(I) Catalysts Acc. Chem. Res. 2017, 50, 2147– 2158 DOI: 10.1021/acs.accounts.7b00178 (c) Weatherly, C. D.; Alderson, J. M.; Berry,

J. F.; Hein, J.; Schomaker, J. M. Catalyst-Controlled Nitrene Transfer by Tuning Metal:Ligand Ratios: Insight into the Mechanisms of Chemoselectivity Organometallics 2017, 36, 1649– 1661 DOI: 10.1021/acs.organomet.7b00190 (d) Huang, M.; Corbin, J. R.; Dolan, N. S.; Fry, C. G.; Vinokur, A. A.; Guzei, I. A.; Schomaker, J. M. Synthesis, Characterization, and Variable Temperature NMR Studies of Silver(I) Complexes for Selective Nitrene Transfer Inorg. Chem. 2017, 56, 6725– 6733 DOI: 10.1021/acs.inorgchem.7b00838 (e) Dolan, N. S.; Scamp, R. J.; Yang, T.; Berry, J. F.; Schomaker, J. M. Catalyst-Controlled and Tunable, Chemoselective Silver-Catalyzed Intermolecular Nitrene Transfer: Experimental and Computational Studies J. Am. Chem. Soc. 2016, 138, 14658– 14667 DOI: 10.1021/jacs.6b07981 (f) Scamp, R. J.; Jirak, J. G.; Dolan, N. S.; Guzei, I. A.; Schomaker, J. M. A General Catalyst for Site-Selective C(sp^3)-H Bond Amination of Activated Secondary over Tertiary Alkyl C(sp^3)-H Bonds Org. Lett. 2016, 18, 3014– 3017 DOI: 10.1021/acs.orglett.6b01392 (g) Rigoli, J. W.; Weatherly, C. D.; Alderson, J. M.; Vo, B. T.; Schomaker, J. M. Tunable, Chemoselective Amination via Silver Catalysis J. Am. Chem. Soc. 2013, 135, 17238– 17241 DOI: 10.1021/ja406654y

31 (a) Martins, L. M. D. R. S. C-Homoscorpionate Oxidation Catalysts- Electrochemical and Catalytic Activity Catalysts 2017, 7, 12 DOI: 10.3390/catal7010012 (b) Wathier, M.; Love, J. A. Hydroelementation of unsaturated C-C bonds Catalyzed by Metal Scorpionate Complexes Eur. J. Inorg. Chem. 2016, 2016, 2391– 2402 DOI: 10.1002/ejic.201501272

32 Liang, S.; Jensen, M. P. Half Sandwich scorpionates as nitrene transfer catalysts Organometallics 2012, 31, 8055– 8088 DOI: 10.1021/om3009102

33 Gardinier, J. R.; Treleven, A. R.; Meise, K. J.; Lindeman, S. V. Accessing Spin-Crossover Behaviour in Iron(II) complexes of N-Confused Scorpionate Ligands Dalton Trans. 2016, 45, 12639– 12643 DOI: 10.1039/C6DT01898J

34 Carrión, M. C.; Jalon, F. A.; Manzano, B. R.; Rodríguez, A. M.; Sepúlveda, F.; Maestro, M. (Arene)ruthenium(II) Complexes Containing Substituted Bis(pyrazolyl)methane Ligands – Catalytic Behaviour in Transfer Hydrogenation of Ketones Eur. J. Inorg. Chem. 2007, 2007, 3961– 3973 DOI: 10.1002/ejic.200700267

35 (a) Evans, D. F. The determination of the paramagnetic susceptibility of substances in solution by nuclear magnetic resonance J. Chem. Soc. 1959, 2003– 2005 DOI: 10.1039/jr9590002003 (b) Evans, D. F.; Fazakerley, G. V.; Phillips, R. F. Organometallic compounds of bivalent europium, ytterbium, and samarium J. Chem. Soc. A 1971, 1931– 1934 DOI: 10.1039/j19710001931 (c) Piguet, C. Paramagnetic Susceptibility by NMR: The ″Solvent Correction″ Removed for Large Paramagnetic Molecules J. Chem. Educ. 1997, 74, 815– 816 DOI: 10.1021/ed074p815

36 Morrison, G.; zur Loye, H.-C. Simple correction for the sample shape and radial offset effects on SQUID magnetometers: Magnetic measurements on Ln_2O_3 (*Ln*=Gd, Dy, Er) standards J. Solid State Chem. 2015, 221, 334– 337 DOI: 10.1016/j.jssc.2014.10.026

37 Bain, G. A.; Berry, J. F. Diamagnetic Corrections and Pascal's Constants J. Chem. Educ. 2008, 85, 532– 536 DOI: 10.1021/ed085p532

38 Ozawa, T.; Kurahashi, T.; Matsubara, S. [3 + 2] Cycloaddition of Aziridines and Alkenes Catalyzed by a Cationic Manganese Porphyrin Synlett 2013, 24, 2763– 2767 DOI: 10.1055/s-0033-1340012

39 Agilent Technologies. CrysAlisPro, version 1.171.34.46 (release 25-11-2010 CrysAlis171.NET; compiled Nov 25, 2010, 17:55:46).
40 Dolomanov, O. V.; Bourhis, L. J.; Gildea, R. J.; Howard, J. A. K.; Puschmann, H. OLEX2: a complete structure solution, refinement and analysis program J. Appl. Crystallogr. 2009, 42, 339– 341 DOI: 10.1107/S0021889808042726
41 Sheldrick, G. M. SHELXTL, version 6.12; Bruker Analytical X-ray Systems, Inc.: Madison, WI, 2001.
42 (a) The, K. I.; Peterson, L. K. Synthesis And Characterization Of Dipyrazolylalkanes, And Some Of Their Complexes With Cobalt(II) Chloride Can. J. Chem. 1973, 51, 422– 426 DOI: 10.1139/v73-062 (b) The, K. I.; Peterson, L. K.; Kiehlmann, E. Preparation Of 1,1′-Carbonyl- And 1,1′-Sulfinyldipyrazoles And Their Reactions With Carbonyl Compounds Can. J. Chem. 1973, 51, 2448– 2451 DOI: 10.1139/v73-366 (c) Peterson, L. K.; Kiehlmann, E.; Sanger, A. R.; The, K. I. Mechanism of The Transition Metal-Catalyzed Reaction Of 1,1′-Carbonyldipyrazoles With Aldehydes And Ketones Can. J. Chem. 1974, 52, 2367– 2374 DOI: 10.1139/v74-343
43 Gowda, B. T.; Jyothi, K.; D'Souza, J. D. Infrared and NMR Spectra of Arylsulphonamides, 4 X-C6H4SO2NH2 and i-X, j-YC6H3SO2NH2 (X = H; CH3; C2H5; F; Cl; Br; I or NO2 and i-X, j-Y = 2,3-(CH3)2; 2,4-(CH3)2; 2,5- (CH3)2; 2-CH3, 4-Cl; 2-CH3, 5-Cl; 3-CH3, 4-Cl; 2,4-Cl2 or 3,4-Cl2) Z. Naturforsch., A: Phys. Sci. 2002, 57, 967– 973 DOI: 10.1515/zna-2002-1210
44 Liddle, B. J.; Hall, D.; Lindeman, S. V.; Smith, M. D.; Gardinier, J. R. Manipulating Self-assembly in Silver(I) Complexes of 1,3-Di(N-pyrazolyl)organyls Inorg. Chem. 2009, 48, 8404– 8414 DOI: 10.1021/ic900982m
45 Reger, D. L.; Semeniuc, R. F.; Little, C. A.; Smith, M. D. Crystal Retro-Engineering: Structural Impact on Silver(I) Complexes with Changing Complexity of Tris(pyrazolyl)methane Ligands Inorg. Chem. 2006, 45, 7758– 7769 DOI: 10.1021/ic0606936
46 Pilar Carranza, M.; Manzano, B. R.; Jalón, F.; Rodriguez, A. M.; Santos, L.; Moreno, M. Experimental and Theoretical Evidence of Unsupported Ag-Ag Interactions in Complexes with Triazine-based ligands. Subtle Effects of the Symmetry of the triazine Substituents New J. Chem. 2013, 37, 3183– 3194 DOI: 10.1039/c3nj00738c
47 Wen, M.; Munakata, M.; Suenaga, Y.; Kuroda-Sowa, T.; Maekawa, M.; Kodai, I. Dinuclear silver(I) complexes of N, N -dibenzyl-4,13-diaza-18-crown-6-ether and dibenzo-24-crown-8-ether Polyhedron 2004, 23, 2117– 2123 DOI: 10.1016/j.poly.2004.03.026
48 Reineke, M. H.; Sampson, M. D.; Rheingold, A. L.; Kubiak, C. P. Synthesis and Structural Studies of Nickel(0) Tetracarbene Complexes with the Introduction of a New Four-Coordinate Geometric Index, τ_δ Inorg. Chem. 2015, 54, 3211– 3217 DOI: 10.1021/ic502792q
49 Gardinier, J. R.; Hewage, J. S.; Lindeman, S. V. Isomer Dependence in the Assembly and Lability of Silver(I) Trifluoromethanesulfonate Complexes of the Heteroditopic Ligands 2-, 3-, and 4-[di(1H-pyrazolyl)methyl]phenyl(di-p-tolyl)phosphine Inorg. Chem. 2014, 53, 12108– 12121 DOI: 10.1021/ic5019357

50 Davis, T. L.; Watts, J. L.; Brown, K. J.; Hewage, J. S.; Treleven, A. R.; Lindeman, S. V.; Gardinier, J. R. Structural Classification of Metal Complexes with Three-Coordinate Centres Dalton Trans. 2015, 44, 15408– 15412 DOI: 10.1039/C5DT02773J
51 (a) Casarin, M.; Forrer, D.; Garau, F.; Pandolfo, L.; Pettinari, C.; Vittadini, A. Tris(pyrazol-1-yl)borate and Tris(pyrazol-1-yl)methane: A DFT study of their different Binding Capability toward Ag(I) and Cu(I) cations Inorg. Chim. Acta 2009, 362, 4358– 4364 DOI: 10.1016/j.ica.2009.02.004 (b) Casarin, M.; Forrer, D.; Garau, F.; Pandolfo, L.; Pettinari, C.; Vittadini, A. Density Functional Theory Study of the Binding Capability of Tris(Pyrazol-1-yl)methane Toward Cu(I) and Ag(I) Cations J. Phys. Chem. A 2008, 112, 6723– 6731 DOI: 10.1021/jp801902c
52 (a) Grochala, W.; Cyranski, M. K.; Derzsi, M.; Michalowski, T.; Malinowski, P. J.; Mazej, Z.; Kurzydlowski, D.; Kozminski, W.; Budzianowski, A.; Leszczynski Crystal and electronic structure, lattice dynamics and thermal properties of Ag(I)(SO_3)R (R = F, CF_3) Lewis acids in the solid state Dalton Trans. 2012, 41, 2034– 2047 DOI: 10.1039/C1DT11747E (b) Johnston, D. H.; Shriver, D. F. Vibrational Study of the Trifluoromethanesulfonate Anion: Unambiguous Assignment of the Asymmetric Stretching modes Inorg. Chem. 1993, 32, 1045– 1047 DOI: 10.1021/ic00058a050 (c) Lawrance, G. A. Coordinated Trifluoromethanesulfonate and Fluorosulfate Chem. Rev. 1986, 86, 17– 33 DOI: 10.1021/cr00071a002
53 (a) Camp, A. M.; Kita, M. R.; Grajeda, J.; White, P. S.; Dickie, D. A.; Miller, A. J. M. Mapping the Binding Modes of Hemilabile Pincer–Crown Ether Ligands in Solution Using Diamagnetic Anisotropic Effects on NMR Chemical Shift Inorg. Chem. 2017, 56, 11141– 11150 DOI: 10.1021/acs.inorgchem.7b01485 (b) Aldrich, K. E.; Billow, B. S.; Holmes, D.; Bemowski, R. D.; Odom, A. L. Weakly Coordinating yet Ion Paired: Anion Effects on an Internal Rearrangement Organometallics 2017, 36, 1227– 1237 DOI: 10.1021/acs.organomet.6b00839 (c) Ward, W. M.; Farnum, B. H.; Siegler, M.; Meyer, G. J. Chloride Ion-Pairing with Ru(II) Polypyridyl Compounds in Dichloromethane J. Phys. Chem. A 2013, 117, 8883– 8894 DOI: 10.1021/jp404838z (d) Ammer, J.; Nolte, C.; Karaghiosoff, K.; Thallmair, S.; Mayer, P.; de Vivie-Riedle, R.; Mayr, H. Ion-pairing of phosphonium salts in solution: C-H···halogen and C-H···π hydrogen bonds Chem. - Eur. J. 2013, 19, 14612– 14630 DOI: 10.1002/chem.201204561 (e) Kleinpeter, E.; Koch, A.; Sahoo, H. S.; Chand, D. K. Tetrahedron 2008, 64, 5044– 5050 DOI: 10.1016/j.tet.2008.03.063 (f) Sahoo, H. S.; Chand, D. K.; Mahalakshmi, S.; Hedayetullah Mir, M.; Raghunathan, R. Manifestation of diamagnetic chemical shifts of proton NMR signals by an anisotropic shielding effect of nitrate anions Tetrahedron Lett. 2007, 48, 761– 765 DOI: 10.1016/j.tetlet.2006.12.002 (g) Macchioni, A. Ion-Pairing in Transition Metal Chemistry Chem. Rev. 2005, 105, 2039– 2073 DOI: 10.1021/cr0300439 (h) La Mar, G. N. Isotropic Shifts of Some Ionic Complexes of Cobalt(II) and Nickel(II): Evidence for Ion Pairing J. Chem. Phys. 1964, 41, 2992 DOI: 10.1063/1.1725664
54 (a) Miras, H. N.; Wilson, E. F.; Cronin, L. Unravelling the complexities of inorganic and supramolecular self-assembly in solution with electrospray and cryospray mass spectrometry Chem. Commun. 2009, 1297– 1311 DOI: 10.1039/b819534j (b) Baytekin, B.; Baytekin, H. T.; Schalley, C. A. Mass spectrometric studies of non-covalent compounds: why supramolecular chemistry in the gas phase? Org. Biomol. Chem. 2006, 4, 2825 DOI: 10.1039/b604265a

55 (a) Banerjee, S.; Mazumdar, S. Electrospray Ionization Mass Spectrometry: A Technique to Access the Information Beyond the Molecular Weight of the Analyte Int. J. Anal. Chem. 2012, 2012, 1 DOI: 10.1155/2012/282574 Schalley, C. A. Molecular Recognition and Supramolecular Chemistry in the Gas Phase Mass Spectrom. Rev. 2001, 20, 253– 309 DOI: 10.1002/mas.10009 (c) Loo, J. A. Electrospray Ionization Mass Spectrometry: A Technology for Studying Noncovalent Macromolecular Complexes Int. J. Mass Spectrom. 2000, 200, 175– 186 DOI: 10.1016/S1387-3806(00)00298-0 (d) Smith, R. D.; Light-Wahl, K. J. The Observation of Non-covalent Interactions in solution by Electrospray Ionization Mass Spectrometry: Promises, Pitfalls and Prognosis Biol. Mass Spectrom. 1993, 22, 493– 501 DOI: 10.1002/bms.1200220902 (e) Su, C. – Y.; Cai, Y.-P.; Chen, C. – L.; Smith, M. D.; Kaim, W.; zur Loye, H. C. J. Am. Chem. Soc. 2003, 125, 8595– 8613 DOI: 10.1021/ja034267k

56 (a) Reger, D. L.; Watson, R. P.; Gardinier, J. R.; Smith, M. D. Impact of Variations in Design of Flexible Bitopic Bis(pyrazolyl)methane Ligands and Counterions on the Structures of Silver(I) Complexes: Dominance of Cyclic Dimeric Architecture Inorg. Chem. 2004, 43, 6609– 6619 DOI: 10.1021/ic0491377 (b) Reger, D. L.; Gardinier, J. R.; Semeniuc, R. F.; Smith, M. D. Silver complexes of 1,1′,3,3′-tetrakis(pyrazol-1-yl)propane: the “quadruple pyrazolyl embrace” as a supramolecular synthon J. Chem. Soc., Dalton Trans. 2003, 1712– 1718 DOI: 10.1039/b301635h (c) Reger, D. L.; Gardinier, J. R.; Christian Grattan, T.; Smith, M. R.; Smith, M. D. Synthesis of the silver(I) complex of $CH_2[CH(pz^{4Et})_2]_2$ containing the unprecedented $[Ag(NO_3)_4]^{3-}$ anion: A general method for the preparation of 4-(alkyl)pyrazoles New J. Chem. 2003, 27, 1670– 1677 DOI: 10.1039/B307306H (d) Reger, D. L.; Foley, E. A.; Semeniuc, R. F.; Smith, M. D. Structural Comparisons of Silver(I) Complexes of Third- Generation Ligands Built from Tridentate (o- $C6H4[CH2OCH2C(pz)_3]_2$) versus Bidentate Poly(1- pyrazolyl) methane Units (o- $C6H4[CH2OCH2CH(pz)_2]_2$) (pz = Pyrazolyl Ring) Inorg. Chem. 2007, 46, 11345– 11355 DOI: 10.1021/ic7017743 (e) Reger, D. L.; Semeniuc, R. F.; Rassolov, V.; Smith, M. D. Supramolecular Structural Variations with Changes in Anion and Solvent in Silver(I) Complexes of a Semirigid, Bitopic Tris(pyrazolyl) methane Ligand Inorg. Chem. 2004, 43, 537– 554 DOI: 10.1021/ic035207i

57 (a) Reger, D. L.; Gardinier, J. R.; Smith, M. D. Tuning the Coordination Geometry of Silver in Bis(pyrazolyl)alkane Complexes Inorg. Chem. 2004, 43, 3825– 3832 DOI: 10.1021/ic0497174 (b) Reger, D. L.; Foley, E. A.; Smith, M. D. Mononuclear Metallacyclic Silver(I) Complexes of Third Generation Bis(1-pyrazolyl)methane Ligands Inorg. Chem. 2009, 48, 936– 945 DOI: 10.1021/ic801594q (c) Reger, D. L.; Watson, R. P.; Smith, M. D. Silver(I) complexes of fixed, polytopic bis(pyrazolyl)methane ligands: influence of ligand geometry on the formation of discrete metallacycles and coordination polymers Inorg. Chem. 2006, 45, 10077– 10087 DOI: 10.1021/ic0613053

58 Reger, D. L.; Gardinier, J. R.; Grattan, T. J.; Smith, M. D. Tricarbonylmanganese(I) derivatives of [Di(pyrazolyl)(2-pyridyl)methyl]aryl Scorpionates J. Organomet. Chem. 2005, 690, 1901– 1912 DOI: 10.1016/j.jorganchem.2004.10.049

59 (a) Niesel, J.; Pinto, A.; Peindy N’Dongo, H. W.; Merz, K.; Ott, I.; Gust, R.; Schatzschneider, U. Photoinduced CO release, cellular uptake and cytotoxicity of a tris(pyrazolyl)methane (tpm) manganese tricarbonyl complex Chem. Commun. 2008, 0, 1798– 1800 DOI: 10.1039/b719075a (b) Pfeiffer, H.; Rojas, A.; Niesel, J.; Schatzschneider, U. Sonogashira and “Click” reactions for the N-terminal and side-chain functionalization of

peptides with $[Mn(CO)_3(tpm)]^+$-based CO releasing molecules (tpm = tris(pyrazolyl)methane) Dalton Trans. 2009, 4292– 4298 DOI: 10.1039/b819091g (c) Pai, S.; Hafftlang, M.; Atongo, G.; Nagel, C.; Niesel, J.; Botov, S.; Schmalz, H.-G.; Yard, B.; Schatzschneider, U. New modular manganese(I) tricarbonyl complexes as PhotoCORMs: in vitro detection of photoinduced carbon monoxide release using COP-1 as a fluorogenic switch-on probe Dalton Trans. 2014, 43, 8664– 8678 DOI: 10.1039/c4dt00254g

60 Feng, J. – J.; Zhang, J. Synthesis of Unsaturated N-Heterocycles by Cycloadditions of Aziridines and Alkynes ACS Catal. 2016, 6, 6651– 6661 DOI: 10.1021/acscatal.6b02072 (b) Wender, P. A.; Strand, D. Cyclocarboamination of Alkynes with Aziridines: Synthesis of 2,3-Dihydropyrroles by a Catalyzed Formal [3 + 2] Cycloaddition J. Am. Chem. Soc. 2009, 131, 7528– 7529 DOI: 10.1021/ja901799s

61 Maeda, R.; Ishibashi, R.; Kamaishi, R.; Hirotaki, K.; Furuno, H.; Hanamoto, T. $AgSbF_6$-Promoted Cycloaddition Reaction of 2-Trifluoromethyl-N-Tosylaziridine with Aldehydes Org. Lett. 2011, 13, 6240– 6243 DOI: 10.1021/ol202697y

62 Kaicharla, T.; Jacob, A.; Gonnade, R. G.; Biju, A. T. AgOTf-Catalyzed dehydrative [3 + 2] Annulation of Azridines with 2-Napthols Chem. Commun. 2017, 53, 8219– 8222 DOI: 10.1039/C7CC03425C

63 (a) Blake, A. J.; Radek, C.; Schröder, M. Tetra(n-butyl)ammonium Trifluoromethanesulfonate Acta Crystallogr., Sect. C: Cryst. Struct. Commun. 1993, 49, 1652– 1654 DOI: 10.1107/S0108270193001544 (b) Leclercq, L.; Suisse, I.; Nowogrocki, G.; Agbossou-Niedercorn, F. On the solid state inclusion of tetrabutylammonium cation in the imidazolium/trifluoromethanesulfonate H-bonds network observed in ionic co-crystals J. Mol. Struct. 2008, 892, 433– 437 DOI: 10.1016/j.molstruc.2008.06.025

Supporting Information

The Supporting Information is available free of charge on the ACS Publications website at DOI: 10.1021/acs.inorgchem.7b02927.

- Tables of crystal data and structure refinement details, supramolecular structures, and details of DOSY and other NMR experiments (PDF)

- PDF